Fall 2023

Electric Freight Transportation System Planning and Truck Operation Optimizations

Xuanke Wu

ELECTRIC FREIGHT TRANSPORTATION SYSTEM PLANNING AND TRUCK OPERATION OPTIMIZATIONS

by

Xuanke Wu

Bachelor of Science.
Hefei University of Technology, 2017

Master of Science.
Central South University, 2020

Submitted in Partial Fulfillment of the Requirements

For the Degree of Doctor of Philosophy in

Civil Engineering

College of Engineering and Computing

University of South Carolina

2023

Accepted by:

Yuche Chen, Major Professor

Yu Qian, Committee Member

Erfan Goharian, Committee Member

Qi Luo, Committee Member

Ann Vail, Dean of the Graduate School

DEDICATION

To mom and dad, Rujuan Hu and Jiwen Wu, who gave me life and taught me optimism, persistence, and humility. And to my girlfriend, fiancée, and future wife, He Zhao.

ACKNOWLEDGEMENTS

First and foremost, I would like to express my sincere gratitude to my Ph.D. advisor, Dr. Yuche Chen, for his unwavering support throughout my academic research and personal development during my Ph.D. program at the University of South Carolina. Under Dr. Chen's guidance, I had the privilege of collaborating with many distinguished and respected professors on various research topics, all of which have significantly contributed to the completion of this dissertation. Dr. Chen's mentorship and support also enabled me to conduct a graduate research grant fully sponsored by the USC graduate school, participate in a wide range of professional conferences, and have my research recognized by fellow scholars, including the Transportation Research Board (TRB) and the American Society of Civil Engineers (ASCE). All of these experiences have unquestionably broadened my horizons and played a pivotal role in shaping my future career and personal development.

Besides, I would like to give my sincere thanks to the committee: Dr. Yu Qian and Dr. Qi Luo have been mentoring me with two of the chapters in this dissertation together with Dr. Chen and helped me a lot with the journal paper writing and revisions. Dr. Yu Qian and Dr. Erfan Goharian also served as committee members during my Ph.D. qualifying test.

Many thanks to Dr. Ruixiao Sun, Dr. Li Ai, Dr. Junlin Ou, Dr. Yunteng Zhang, and Dr. Feng Guo (the names listed in the Acknowledgment are presented in no particular order), not only for all the insightful discussions on the research, but also for

sharing your experiences on how to deal with relationship difficulties. I also would like to thank and Dr. Ning Li and Dr. Zhonghua Yang, who helped me a lot with my accommodation and vehicles. It was a great pleasure to get to know with them when I just came to the United States in 2019.

I greatly acknowledge the funding received toward this dissertation from the National Science Foundation under Award (FAIN) 2213731, the Federal Railroad Administration (FRA) with the Contract No. 693JJ621C000015 and the Support to Promote Advancement of Research and Creativity (SPARC) Graduate Research Grandt from the University of South Carolina with the proposal No. 155200-23-62590.

I would owe a big thank you to all those who have lived and worked with me during my Ph.D. program, especially for Yihong Ning, who is currently working in my group. Thanks to Hung-Tien Huang for his help with my auto problems and sharing rides with me at the beginning of my arrival, who is always either meowing or on his way to meow like a cat anywhere he is. Thanks to future professors and who are currently working in Dr. Yu Qian's and Dr. Yi Wang's academic families, thanks Yufeng Gong, Shihao Huang, Youzhi Tang, Ge Song, Yichuan Cao, Jiawei Guo and Huaqiang Guo for the great moments we hung out together.

There are also a bunch of American friends who have helped me a lot during recent years. Thanks Ron Parker and Marian Parker for their kindness and worm hospitality whenever I visited the Living Stone Chinese Community Church and Ron's presence at my final defense. Thanks to Scott Andes, Victoria Andes, Keith Cook and Elisabath Cook, Noel and those who are working for Reformed University Fellowship for Internationals (RUF-I), I had a dramatically wonderful time with them for the hiking

trips, English studies, and fun. Thanks to Dr. Raj, Michael Krigline, and those who are working for the International Friendship Ministry (IFM) for organizing Friday night's activities, which enriched my life after school. Thanks to Steve Bostrom and John Myers for their consistent efforts in providing high-quality weekly English materials and enhancing my spoken English skills.

I owe my deepest gratitude to my parents, Jiwen Wu and Rujuan Hu, for their unconditional love and mental support. Last but certainly not least, I extend my deepest and heartfelt gratitude to my girlfriend, He Zhao, whom I have known since October 2013. Here's to a joyful celebration of our tenth anniversary of acquaintance for both you and me. Hand in hand while we are growing older together.

ABSTRACT

The substantial demand for fossil fuel consumption is a significant contributor to greenhouse gas emissions, drawing considerable public attention to health and environmental problems. As a result, vehicle electrification is currently recognized as the most effective approach to reduce CO_2 emissions from transportation. However, compared to traditional fossil fuel-powered vehicles, electric vehicles have notable disadvantages, including higher upfront purchasing price, longer recharging time, and most significantly, lower driving ranges. All these challenges can potentially result in increased overall operational costs for logistics companies.

This thesis proposes a comprehensive optimization modeling framework for electric freight transportation system planning and operations with a particular focus on its applicability to outbound logistics. Outbound logistics addresses the demand side of the supply-demand equation, involving the storage and transportation of goods from initial hubs or warehouses to the end customer or user. An empirical study is first conducted to scrutinize the extra time spent on charging-related activities by employing electric drayage trucks at the San Pedro Port of Los Angeles (POLA) and Port of Long Beach (POLB) in the State of California. By showing the proportion of time spent on charging, the author argues that the operation efficiency can be significantly improved by offering alternative battery charging options. The second part of the thesis explores the Vehicle Routing Problem (VRP) for electric truck platoons equipped with trailers, assuming that trailer batteries can be replaced at specific locations. Specifically, the

system planning optimization framework focuses on minimizing system costs by optimizing designated trailer battery exchange locations at the upper level. Simultaneously, at the lower level, the electric truck platoon routing problem is solved, with a trailer battery feeder from the regional depot pre-delivering battery replacements to each exchange location. Finally, this thesis addresses the last mile delivery problem, taking train blockages into consideration. The proposed framework can significantly improve logistics system efficiency, lower total costs, and enhance the competitiveness of electric trucks compared to traditional fuel-powered vehicles.

TABLE OF CONTENTS

LIST OF TABLES

LIST OF FIGURES

LIST OF SYMBOLS

CHAPTER 3

n Index of time stage in the operational decision process, n={1,…,N}.

i Index of vehicle, i={1,…., y_I}.

a Index of activity decision by vehicles, a={1: long-distance delivery, 2: middle-distance delivery, 3: short-distance delivery, 4: charging, 5: idling, 6: a vehicle is on a delivery trip}.

c_I The unit cost associated with the type of truck, $/truck.

c_K The unit cost of building an electric charging station, $/station.

β_n^a a=1, 2, 3: delivery associated cost at stage n, $/hour; a=4, 5: labor cost associated with charging or idling at stage n, $/hour.

ε_n Electricity associated cost at stage n (peak/off-peak hours), $/hour.

γ_i^a a=1, 2, 3: energy consumption associated with deliveries for vehicle i, kWh; a=4: battery energy recovery while charging for vehicle i, kWh.

h_a a=1, 2, 3: required hours for deliveries, hours.

U_i Battery capacity for vehicle i, kWh.

L_i Battery minimum level for vehicle i, kWh.

T_a a=1, 2, 3: required daily throughput for deliveries, TEUs.

$\varphi_c(y_I, y_K)$ Infrastructure cost for y_I electric trucks and y_K charging stations.

$\varphi_g(y_I, y_K)$ Operational cost when daily throughput is met of y_I electric trucks and y_K charging stations.

y_I Decision Variable, total number of trucks to purchase, including large and small.

y_K Decision Variable, total number of electricity chargers to install.

$x_{n,i}^{a}$ Decision Variable, binary, whether vehicle i takes activity decision a at stage n.

$\mathcal{S}_n$ State of charge of all vehicles at stage n.

$R_{n,i}$ The remaining hours that vehicle i is out for delivery, specifically, $R_{1,i} = 0$.

CHAPTER 4

I Set of Customers, $i \in I$.

J Set of trailer exchange location candidates, $j \in J$.

K Set of heavy-duty electric truck platoons, $k \in K$.

T Set of trips, $t \in T$.

F Set of trailer battery feeders, $f \in F$.

$\{o, o'\}$ Set of the depot and its copy.

V Set of all nodes, $V = I \cup J \cup \{o, o'\}$.

y_j Decision Variable, binary, $y_j = 1$ if candidate j is a trailer exchange station; otherwise, $y_j = 0$.

$x_{i,j}^{k,t}$ Decision Variable, binary, $x_{i,j}^{k,t} = 1$ if vehicle k goes from node i to node j at t^{th} trip; otherwise, $x_{i,j}^{k,t} = 0$.

$w_{i,j}^{f,t}$ Decision Variable, binary, $w_{i,j}^{f,t} = 1$ if trailer battery feeder f goes from node i to node j at t^{th} trip; otherwise, $w_{i,j}^{f,t} = 0$.

c_j Trailer battery exchange location setup cost at node j, $j \in J$.

d_{ij} Distance between node i and node j, $\forall i, j \in V$.

t_{ij} Traveling time form node i to node j at the designated speed.

ρ_1, ρ_2 Unit labor cost per hour for truck and battery feeder drivers, respectively.

M A large number.

q_i Customer demand at node i, $\forall i \in I$.

U_k Total loading capacity of truck platoon k, $\forall k \in K$.

u_{ikt} The on-vehicle load when vehicle k leaves node i for the t^{th} trip, $\forall k \in K, i \in V, t \in T$.

Q_1, Q_2 The battery driving range for electric tractors and trailers, respectively.

P_{ikt}^1, P_{ikt}^2 The maximum distance that the remaining battery power allows when vehicle k arrives at and leaves node g for the t^{th} trip, respectively, $\forall k \in K, i \in V, t \in T$.

s_k The number of trucks in platoon k, $k \in K$.

CHAPTER 5

$G = (V, A)$ Directed non-negative weighted graph.

V The set of nodes in G, $v \in V$.

A The set of weighted arcs/links, $a_{ij} \in A$.

l_{train} Train length.

v_{train}^t Train operating speed at time t.

$d_{train}^{i,j}$ Train route distance between grade crossing nodes i and j.

$[t_v^s, t_v^e]$ Train blockage window at node v starting at t = t_v^s and ending at t = t_v^e.

(r, s) OD pair, from origin node r to destination node s.

$\bar{t}_{ij}$ The average road traveling time on the arc/link a_{ij}.

b_{ij} A binary variable, $b_{ij} = 1$ if the arc/link a_{ij} is blocked by a train, otherwise, $b_{ij} = 0$.

T_v Accumulative time after an emergency occurs when the emergency vehicle arrives at node *v*.

D_v Expected time delay at node *v*.

D_{total} Total/cumulative time delay of the vehicle.

x_{ij}^{rs} Decision Variable, binary, $x_{ij}^{rs} = 1$ if the link a_{ij} lies on the path (r, s), otherwise, $x_{ij}^{rs} = 0$.

LIST OF ABBREVIATIONS

BSS .....Battery Swap Station

CCL.....Customer Covering List

CSX..... CSX Transportation, Inc.

CVRP .....the Capacitated Vehicle Routing Problem

EHDV .....Electric Heavy-Dfirstuty Vehicles

EV ..... Electric Vehicles

EVRP ..... Electric Vehicle Routing Problem

FAF .....Freight Analysis Framework

FLP .....Facility Location Problem

FRA .....Federal Railroad Administration

GA..... Genetic Algorithm

GDP..... Gross Domestic Product

GHG..... Greenhouse Gas

GPS .....the Global Positioning System

HPC.....High-Performance Computing

LRP ..... Location-and-Routing Problem

MIP .....Mixed Integer Programming

NP-complete ..... Non-deterministic Polynomial time complete

NP-hard.....Non-deterministic Polynomial time hard

NREL .....the National Renewable Energy Laboratory

NSGA-II..... Nondominated Sorting Genetic Algorithm II

OD..... Origin-Destination

OR..... Operations Research

POLA..... Port of Los Angeles

POLB..... Port of Long Beach

SA.....Simulated Annealing

SC..... South Carolina

SOC..... (Battery) State of Charge

SUMO.....Simulation of Urban Mobility

TEU..... Twenty-foot Equivalent Unit

TS..... Tabu Search

VRP.....Vehicle Routing Problem

VRPPD.....Vehicle Routing Problem with Pickup and Delivery

VRPTW.....Vehicle Routing Problem with Time Windows

USPS..... United States Postal Service

CHAPTER 1

INTRODUCTION

1.1. BACKGROUND

Recent statistics show that the United States ranks only behind China in total vehicle production, with more than 290.8 million vehicles registered nationwide in 2022 and its auto industry represents 3% of the total Annual Gross Domestic Product (GDP) ("36 Automotive Industry Statistics [2023]," 2023). Meanwhile, in Figure 1.1, the combustion of fossil fuels such as gasoline and diesel to transport people and goods was the largest source of CO2 emissions in 2021, accounting for 35% of total U.S. CO_2 emissions and 28% of total U.S. greenhouse gas (GHGs) emissions, drawing considerable public attention to health and environmental problems (US EPA, 2023a).

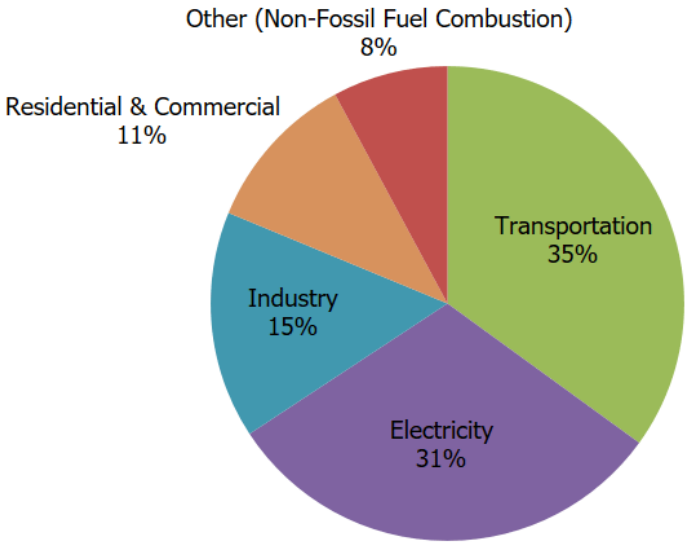

U.S. Environmental Protection Agency (2023). Inventory of U.S. Greenhouse Gas Emissions and Sinks: 1990–2021

Figure 1.1 U.S. carbon dioxide emissions by economic sector.

As a result, vehicle electrification is currently recognized as the most effective approach to reduce CO_2 emissions from transportation. There is a noticeable surge in plug-in electric vehicle sales in the U.S., with expectations that electric vehicle sales may reach or even surpass 50% by 2030 (U.S. Bureau of Labor Statistics, 2023). In 2018, three California ports translated their visions of cleaner air into actions. The State of California has launched a zero-emission truck project and plans to phase out heavy-duty diesel trucks hauling containers to ships and warehouses by 2035, making the ports a focal point for forward-thinking investors eager to build charging stations for electric semis that will ultimately serve these vital trade gateways (Baertlein and Baertlein, 2023; Sandifur, 2021). Indeed, the shift toward vehicle electrification holds the promise of a brighter and more sustainable future. However, it's crucial to acknowledge that this transition process is still facing its challenges. When compared to traditional fossil fuel-powered vehicles, electric vehicles still have notable disadvantages, including higher upfront purchasing price, fewer supporting facilities, longer recharging time, and most significantly, lower driving ranges (Figure 1.2). All these disadvantages can potentially result in increased overall operational costs for logistics companies and finally affect the popularity of electric trucks in the market.

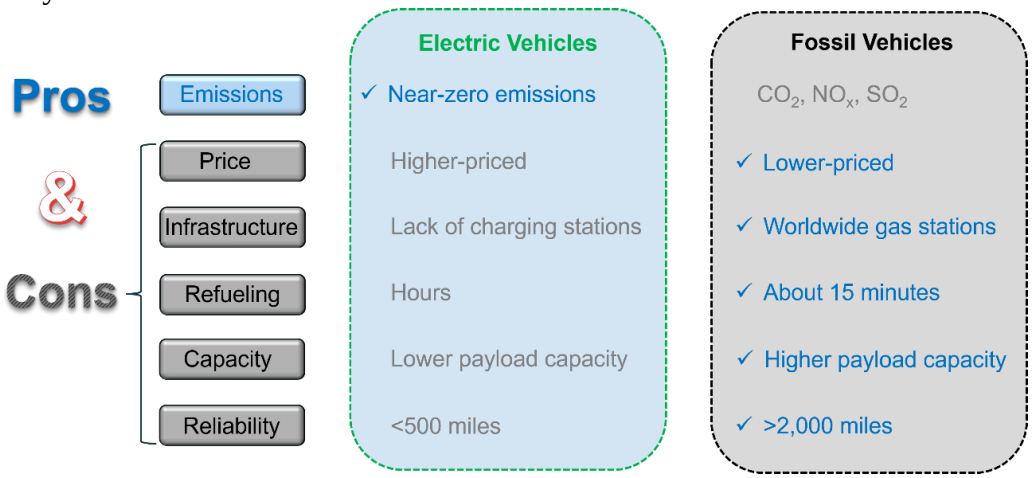

Figure 1.2 Electric V.S. diesel trucks.

There is a body of literature dedicated to managing and operating electric cars and their charging infrastructure with optimization methods, aiming to enhance the performance of electric vehicles. Numerous studies have investigated routing problems in various real-world scenarios, with the goal of maximizing passenger flow while minimizing fleet size and operating costs. Specifically, many of these studies have addressed the mileage range challenges for electric cars in passenger transportation, taking into account factors such as driving range and charging features (Hurtado-Beltran et al., 2021; Mohamed et al., 2022; Montoya et al., 2017a; Whitehead et al., 2022) and some other studies have focused on developing routing strategies that consider charging functions (Dessouky and Yao, 2023; Felipe et al., 2014; Hiermann et al., 2016; Jiang et al., 2018; Kim and Chung, 2023).

From the above observations, it becomes evident that infrastructure planning and operation scheduling are essential for electric trucks, especially to effectively adapt to long-haul transportation. Nevertheless, most of the existing studies listed above focus on one particular transportation segments, and no one has attempted to optimize infrastructure planning and vehicle operations from the perspective of the entire logistics system, spanning from initial transportation hubs to final customers. Therefore, this thesis separates the entire logistics process into sections (Figure 1.3), and each section will solve one of the real-world implementation problems. Specifically, the first research focuses on the goods delivery from initial hubs to reginal depots with traditional charging options, i.e., the charging facilities are limited, decision makers have to optimize the operating and charging schedules of the electric trucks to realize the minimum system cost.

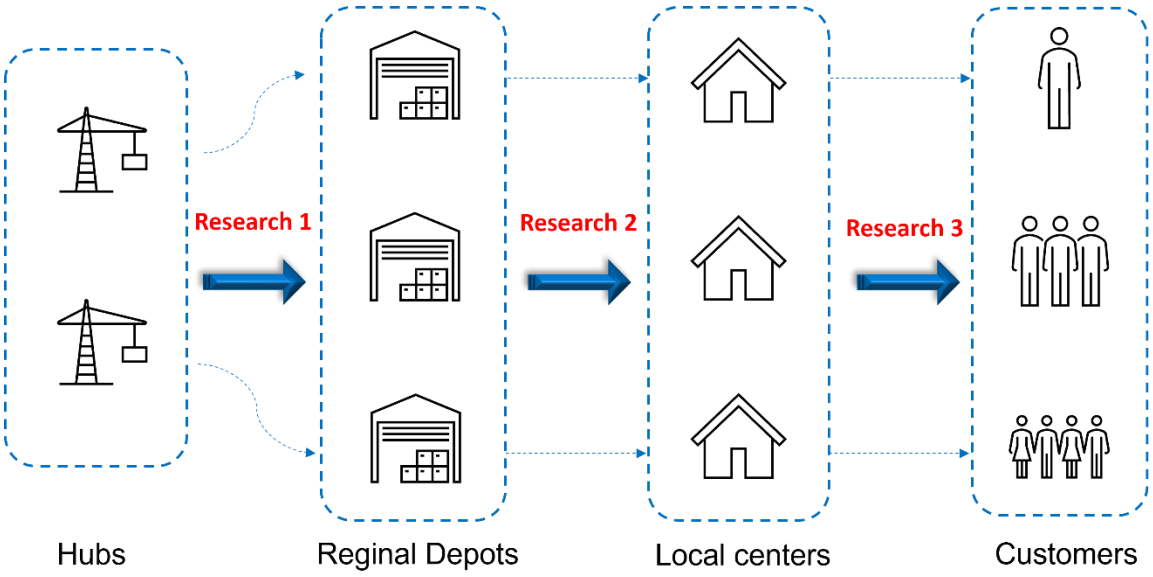

Figure 1.3 Research framework.

Another question that is usually neglected by previous research is the feasibility of offering alternative charging options to electric vehicles, potentially saving a significant amount of charging time, rather than relying solely on on-the-spot physical charging. With the results obtained from the first research, conclusions can be drawn that even with highly advanced optimization methods, there will still be a certain amount of time that electric trucks remain idling due to the need for battery charging. Consequently, the second research aims to explore alternative options for battery charging to improve the operation efficiency of electric trucks while processing goods from regional depots to local centers.

The third research deals with the last mile delivery problem. Although the shortest path problem and its diverse variants have been extensively studied in numerous scenarios (Bertsekas, 1993; Carrabs et al., 2020; Chassein et al., 2019; Desaulniers et al., 2014; Di Puglia Pugliese et al., 2020; Dreyfus, 1969), there is a gap in research when it comes to investigating shortest path planning while considering train blockages. Such considerations can fundamentally alter the commonly recommended shortest routes

suggested by the shortest path algorithms above or advanced navigation technics such as Google Maps.

1.2 PROBLEM STATEMENT AND RESEARCH GOALS

The overarching goal of the thesis is to optimize freight transportation system planning and logistic operations while minimizing overall system costs, specifically in response to the emerging trend of non-emission truck electrification.

1.2.1 JOINT OPTIMIZATION FRAMEWORK FOR DRAYAGE TRUCKS AT PORTS

Drayage trucks refers to trucks that operate near ports. Though studies focused on minimizing charging costs by optimizing recharging schedules and specifications of charging are interesting (Paul and Yamada, 2014; Teichert et al., 2019; Wang et al., 2017), they do not apply to drayage truck planning and operating optimization, because drayage truck operation has challenges in 1) sequential decision making, given that drayage trucks must frequently move between locations in port areas; 2) freight transportation is different from passenger transportation because the goods are normally heterogeneous products and require different transport truck types and movement distances can vary significantly. In this study, the author contributes to

- a novel approach with sequential daily operational decisions to addressing the knowledge gap in the literature surrounding the deployment of electric drayage trucks in port areas.
- the development of a robust mathematical optimization framework capable of determining intra-day trips and charging activities for trucks of various battery sizes.

1.2.2 TRAILER BATTERY EXCHANGE FOR MIDDLE-MILE TRUCK FLEETS

While earlier studies have predominantly concentrated on developing battery technology for electric heavy-duty vehicles (EHDVs) (Budde-Meiwes et al., 2013; Ma et al., 2021; Manthiram, 2017; Manzetti and Mariasiu, 2015; Soloveichik, 2011; Young et al., 2013), greater emphasis needs to be placed on resolving logistical and operational challenges in highway systems. Compared to traditional strategies that involve recharging at depots or specific charging stations, the battery swapping method offers the advantage of time-saving and becomes a promising solution to alleviate "range anxiety" for EHDVs (Li, 2014; Yang and Sun, 2015). In this research, the author contributes to

- a novel and more flexible trailer battery exchanging approach to address the electric truck “range anxiety” problem, with significant time savings from battery charging.
- a bi-level mathematical model for the electric truck routing problem, solving the trailer exchange location and route optimization simultaneously.

1.2.3 LAST MILEDELIVERY ROUTING PROBLEM WITH TRAIN BLOCKAGES

A grade crossing is where a railway and a road cross at the same level. In 2015, the FRA acknowledged that complaints regarding blocked crossings ranked as the most common type of complaint they received (Njus, 2016). Although many studies have been conducted on shortest path problems with time window constraints (Di Puglia Pugliese et al., 2020; El-Sherbeny, 2014; Sancho, 1994), they have yet to investigate the shortest path problems with train blockages. Recognizing the substantial impact of blocked grade crossings, this research contributes to

- a framework that mitigates such disruptions and enhances the time efficiency of the last mile deliveries, ensuring that they are not impeded by passing trains.
- a dynamic train blockage window estimation method using updated train GPS data.

1.3 DISSERTATION OUTLINE

The remainder of the thesis is organized as follows. Chapter 2 provides an overview of the current research on electric transportation system infrastructure planning (e.g., locations of reginal and local hubs, number and locations of charging stations, truck fleet size, etc.), electric truck operation scheduling and vehicle routing planning methods, along with existing literature on shortest path problems, providing readers with a general idea of how this thesis fits into the big picture. Chapter 3 solves port system infrastructure planning and electric drayage truck operation problems, delivering containers from initial hubs to reginal depots with traditional charging methods. Chapter 4 discusses the alternative charging options for middle-mile electric truck fleets, transporting goods from reginal depots to local distribution centers through highway systems. Chapter 5 deals with the last mile delivery routing planning problem within an urban road network with potential train blockages.

CHAPTER 2

LITERATURE REVIEW

In response to the growing challenge of GHG emissions, the California Air Resources Board approved the Advanced Clean Fleets Regulation in April, 2023, indicating that starting 2024, all new drayage trucks are required to be zero-emissions and the entire drayage fleet being zero-emissions by 2035 ("Advanced Clean Fleets Regulation - Drayage Truck Requirements | California Air Resources Board," 2023).

As truck electrification gains prominence as a solution for transportation emissions, more attention is being directed toward electric charging system planning and electric vehicle operations.

2.1 ELECTRC TRUCK SYSTEM PLANNING AND MANAGEMENT

There is a body of literature focusing on managing and operating electric cars and their charging infrastructure. Many studies look at the routing problems of electric cars in various real-world settings. The objectives of these studies are to maximize passenger flow and minimize fleet size and operating costs. Particularly, considering electric cars' driving range and charging features, these studies proposed various methods to solve the mileage range challenges for electric cars for passenger transportation. Some studies focused on designing routing strategies considering charging functions (Felipe et al., 2014; Hiermann et al., 2016; Jiang et al., 2018; Schneider et al., 2014a; Zhang et al., 2018). For example, Montoya et al (Montoya et al., 2017a) extended classical electric vehicle routing problems

to consider non-linear charging functions, i.e., state of charge level is not linearly increased with charging time. They developed a mixed-integer programming method and converted the non-linear feature of charging into a series of linear constraints. Other studies investigated assigning electric vehicles for predetermined routes considering charging facility locations (Ke et al., 2016; Li, 2014; Wen et al., 2016). And yet other studies focused on minimizing charging costs by optimizing recharging schedules and specifications of charging, such as charger power and battery size (Paul and Yamada, 2014; Teichert et al., 2019; Wang et al., 2017). Though these studies are interesting, they do not apply to drayage truck planning and operating optimization.

Limited studies studied logistics systems with electric trucks. Sassi and Oulamara (Sassi and Oulamara, 2014), developed models for optimally assigning electric trucks to predetermined routes and scheduling charging activities at a single depot. Vahdani and Shahramfard (Shahram fard and Vahdani, 2019) developed a dual-objective optimization model to solve for assignment of trucks and forklifts for a multidoor, cross-dock problem. Schiffer and Walther (Schiffer and Walther, 2018) developed a robust optimization to coordinate plan charging location and truck routing for freight transportation. They find that the coordinated decision process can improve system performance and reduce system costs. Above relevant studies of electric trucks focus on determining routes and charging locations for long-haul freight transportation. But drayage trucks have features of frequent movements within a confined area (Beard-Raymond et al., 2009). This makes the time-dependent operating decision to be critical in drayage truck fleet management.

2.2 VEHICLE ROUTING PROBLEM

There are mainly two streams of research directly related to this thesis. The first stream investigates the Vehicle Routing Problem (VRP), which is a well-known challenge in Operations Research (OR), involving finding optimal routes to deliver goods to a number of customers from one or more depots (Braekers et al., 2016; Yeun et al., 2008). The classical VRP and its variants, such as the capacitated vehicle routing problem (CVRP), vehicle routing problem with time windows (VRPTW), and vehicle routing problem with pickup and delivery (VRPPD), have been proven to be NP-hard problems (Lenstra and Kan, 1981; Yeun et al., 2008). As a result, heuristic and metaheuristic methods are often more suitable for practical applications, while exact solutions are only efficient for small-scale problems (Braekers et al., 2016; Bräysy et al., 2004; Chiang and Russell, 1996; Choi and Tcha, 2007; Laporte, 1992).

Particularly for electric vehicle routing problems (EVRP), Conrad and Figliozzi firstly introduced recharging VRP in 2011, with load capacity and time window constraints, in which vehicles can get recharged at customer nodes (Conrad and Figliozzi, 2011). Later, Schneider et al. presented capacitated EVRP with time windows and solved the problem with a hybrid algorithm combining a variable neighborhood search and a Tabu Search (TS) heuristic (Schneider et al., 2014b), which has become a basic foundation for the following studies on EVRP (Amiri et al., 2023). To better simulate real-world charging conditions, further works on non-linear charging function has also been investigated since the first model was proposed in 2017 (Lee, 2021; Montoya et al., 2017b; Zuo et al., 2019). Sassi et al. investigated a fixed fleet of EVRP to reduce the number of vehicles and the cost of shipping and recharging, while at the same stage, the domain of EVRP considered a

heterogeneous fleet (Sassi et al., 2014). They have also developed iterated TS and multi-start iterated local search algorithms for solving the fixed fleet EVRPs (Sassi et al., 2015a, 2015b). Some other research has added energy consumption factors to the energy function of the mixed fleet of EVRP, like speed, acceleration, deceleration, road gradients and load weight (Macrina et al., 2019; Sassi et al., 2014). Although taking all these factors into consideration can help better estimate energy consumptions in the real-world conditions, Amiri et al. argued that an average rate per distance is still a good choice to maintain the simplicity of the present study (Amiri et al., 2023).

The second related stream is about Location-and-Routing Problems (LRP). Different from the traditional VRP and its variants only focusing on vehicle routing issues, a basic LRP can be decomposed into two sub-problems: the Facility Location Problem (FLP) and a VRP, where the FLP belongs to the strategic decision level and the decision is valid for a long-term period while the VRP is at the tactical or operational decision level and the decision is only valid for a short period (Mara et al., 2021; Salhi and Nagy, 1999). This natural characteristic accounts for the potential inaccuracy and inflexibility to make instant adjustments to the fluctuating customer demands for most real-world implementations. Lopes et al. and Prodhon and Prins published two surveys that have partially classified the works on LRP (Lopes et al., 2013; Prodhon and Prins, 2014). Previous studies have also demonstrated that traditional approaches that independently optimize these two interconnected problems can lead to suboptimal results. (Mara et al., 2021; Salhi and Rand, 1989). Therefore, recent solutions to LRP are engaged in integrating these two decision levels with the objective of solving location and routing problems simultaneously.

According to the latest survey from Mara et al., metaheuristics are still the most popular option to solve an LRP model. Heuristics such as simulated annealing (SA) and genetic algorithm (GA) are flavored for single objective LRPs, while nondominated sorting genetic algorithm II (NSGA-II) and multi-objective particle swarm optimization are preferred for multi-objective LRPs (Mara et al., 2021). Although the development of exact methods on LRP is relatively more demanding and require special structure of the VRP, there are several well-received approaches or commercial solvers available for LRPs, like GUROBI, CPLEX or LINGO, which also can be referred to (Mara et al., 2021).

2.3 THE SHORTEST PATH PROBLEM

The initial shortest path problems focus on the travel distance and have been successfully addressed with typical route planning algorithms, like Dijkstra's algorithm (Dijkstra, 1959; El-Sherbeny, 2014; Johnson, 1973) label setting approach (Dreyfus, 1969) and Bellman-Ford algorithm (Awerbuch et al., 1994; Schambers et al., 2018). And then, studies on the shortest path problem with time window constraints became a new hot topic in the 1990s, where the time windows indicate the periods when the node or arc is available for service (Di Puglia Pugliese et al., 2020; El-Sherbeny, 2014; Sancho, 1994). Although many studies have been conducted on shortest path problems with time window constraints, they have yet to investigate the shortest path problems with train blockages. And likewise, studies have yet to explore the strategy to dispatch delivery vehicles when the postman deliver packages to customers, considering train blockages in the road network.

Unfortunately, it has been established that the majority of shortest path problems fall into the categories of non-deterministic polynomial time hard (NP-hard) or NP-

complete problems (Carrabs et al., 2020; Chassein et al., 2019; Ferone et al., 2020; Saraiva and de Andrade, 2021; Yu and Yang, 1998; Zhen et al., 2020). This indicates that finding efficient solutions for this class of problems poses significant challenges due to the computational complexity, especially for large-scale/size networks. Table 2.1 provides a comparison between the road network scales examined in the existing literature and the scale considered in this paper. The findings clearly indicate that the network scale investigated in this paper is significantly larger than what has been explored in the existing literature. Therefore, the objective of this study is to develop a practical and time-efficient system that can identify the optimal route for last mile deliveries, taking potential train blockages into account.

Table 2.1 Network scale comparison.

References	**Time window**	**Train blockage**	**# of nodes**	**# of arcs**
Dreyfus, 1969	×	×	5	7
Johnson, 1973	×	×	7	42
Sancho, 1994	√	×	7	12
Güner et al., 2012	×	×	30	98
Festa et al., 2013	×	×	Up to 100	Up to 9,900
Shahabi et al., 2015	×	×	24	78
Wang & Zlatanova, 2016	×	×	1,780	1,586
Chassein et al., 2019	×	×	538	1,308
Shiri & Salman, 2020	×	×	Up to 500	Up to 1,500
Ferone et al., 2020	×	×	Up to 450	Up to 1,710
Carrabs et al., 2020	×	×	6	11
Pugliese et al., 2020	√	×	7	7
Saraiva & de Andrade, 2021	×	×	Up to 350	Up to 900
This dissertation	√	√	7,668	21,502

CHAPTER 3

JOINT OPTIMIZATION OF ELECTRIC DRAYAGE TRUCK OPERATIONS AND CHARGING STATIONS PLANNING AT PORTS[1]

3.1 INTRODUCTION

Cargo shipping has contributed a significant amount of particulate matter, nitro oxide, and sulfur oxide emissions (Eyring et al., 2005; Transportation (ICCT), 2007; Wu et al., 2023) Although most shipping emissions take place at sea, the most directly noticeable aspect, which also generates the most direct health impacts, takes place in port areas and cities (Schrooten et al., 2009). Specifically, drayage trucks at ports contribute significantly to poor air quality in and near port areas (Filippo et al., 2019). Electrification of port drayage fleets is viewed as a promising strategy to reduce emissions at ports (Kim et al., 2012). Trucks can be generally divided into light-duty trucks and heavy-duty trucks. And the electrification process of these two truck types is different. Light-duty trucks refer to trucks with a gross vehicle weighing up to 3,860 kg and a payload capacity of up to 1,815 kg. They are mainly used for transporting passengers and household goods. In the past several years, many car makers have introduced or plan to introduce electric light-duty trucks, such as the electric F-150 by Ford, R1T by Rivian, Hummer EV by General Motors, etc. These electric light-duty trucks have driving ranges between 200 to 350 miles. This is

[1] X. Wu, Y. Zhang and Y. Chen, "A Dynamic Programming Model for Joint Optimization of Electric Drayage Truck Operations and Charging Stations Planning at Ports," in IEEE Transactions on Intelligent Transportation Systems, vol. 24, no. 11, pp. 11710-11719, Nov. 2023, doi: 10.1109/TITS.2023.3285668.

enough for most of the daily usage of light-duty trucks. Therefore, the market experiences an upward trend in the adoption and penetration of light-duty trucks. However, the situation is different for the electric heavy-duty truck market. Heavy-duty trucks refer to trucks with a gross vehicle weight above 12,000 kg and these vehicles are mainly used for long-haul freight (e.g., interstate transportation) and short-haul goods movement (e.g., drayage trucks in port areas). There is a very limited number of electric heavy-duty truck models in the market, including BYD's 8TT, Volvo VNR, Daimler eCascadia, etc. These trucks' driving ranges are between 70-120 miles, with a battery size ranging between 200 to 300 kWh. And most electric heavy-duty trucks that will be introduced by 2030-2035 are having a battery size of at least 500 kWh and a mileage range above 200 miles. The market portfolio of heavy-duty trucks and their battery specification clearly proves that the electricity driving range is a major challenge for the adoption of electric trucks at present time and this is particularly true for the adoption of electric drayage trucks in port areas (Tanvir et al., 2021). There are several port authorities (e.g. Los Angles, Long Beach) considered the deployment of electric drayage trucks in their jurisdictions to solve air quality problems. But they all recognized the driving range limitation and lack of experience in managing the electric truck fleet (Filippo et al., 2019.; Kim et al., 2012). Therefore, efficient planning, managing and operating electric heavy-duty trucks and charging infrastructure is critical to the success of adopting electric trucks in port areas (Çabukoglu et al., 2018; Liimatainen et al., 2019; Lu et al., 2018).

There are limited studies related to drayage truck operations and management. Drayage truck operation has challenges in 1) sequential decision making, given that drayage trucks must frequently move between locations in port areas; 2) freight

transportation is different from passenger transportation because the goods are normally heterogeneous products and require different transport truck types and movement distances can vary significantly. There are some studies related to truck appointment systems for drayage truck operations in ports and Huynh et al. (Huynh et al., 2016) summarized these studies. Drayage truck appointment studies focus on optimally coordinating arrival time among drayage trucks to arrive at port terminals. And most drayage appointment studies focus on the one-time arrival of trucks, which means each truck (normally belonging to different companies) only comes to the terminal one time per day to transport containers. For example, Chen et al. (Chen et al., 2013) developed an integer programming framework to optimally spread the terminal arrival time of a fleet of drayage trucks to reduce waiting time at terminal gates. It does not consider the sequential decision of drayage truck operations. Phan and Kim (Phan and Kim, 2015) proposed a decentralized decision-making model for the terminal to coordinate the arrival time of drayage trucks from different companies. The paper formulated drayage truck negotiations with equilibrium constraints. But the paper still focuses on one-time arrival per day for each drayage truck. The above literature fails to consider sequential decision-making of drayage truck movements within the port terminal during the day. Other relevant studies investigate trip characteristics of drayage trucks. For example, You and Ritchie (You and Ritchie, 2018) analyzed drayage truck driving data in Los Angles Port and showed trip length, trip average speed, and trip types of drayage trucks during a typical day of operation. Prohaska et al. (Prohaska et al., 2016) conducted a similar study on the drayage truck driving behavior of Long Beach Port. These studies provide informative drayage truck driving data, but they do not consider optimizing drayage truck fleet management given the driving data. There is even no

relevant study on electric drayage truck operation and planning optimization. Some studies look at the feasibility of deploying electric drayage trucks and analyzed the installation and operating cost of charging stations at port areas (Filippo et al., 2019.; Kim et al., 2012). These studies provide useful information but are not directly relevant to operation and planning.

Drayage truck operations have specific features on their frequent movements within port areas, which requires sequential decision-making on truck operating and charging activities within a day. Specifically, to make full use of trucks, trucks will pick up several deliveries every single day and then return to the port for new deliveries. Right before taking a new mission, drivers need to consider if the residual energy of the battery can afford the next round trip. If not, then trucks must be charged before new deliveries. Besides, electricity will be charged at different rates depending on the charging time (peak or off-peak hours), which indicates avoiding charging during peak hours can help reduce the total operational cost. Therefore, this is a multi-dimensional sequential decision-making process based on the battery state of charge (SOC) through the whole daily operational stages. Relevant studies on passenger transportation of electric cars/buses do not apply to drayage trucks because transporting passenger and freight goods are different. Relevant studies on electric long-haul trucks are not directly applicable to drayage trucks because those studies normally do not consider time-dependent decisions within a day. Relevant drayage truck studies either focus on appointment systems, or cost-benefit-based feasibility analysis, but they do not evolve the time-sequential decision-making process.

This research fills that knowledge gap by proposing a joint optimization framework to integrate fleet planning and truck operation decisions for the operation of electric

drayage trucks for port electrification. Specifically, the author develops a time-sequential decision-making dynamical programming model to co-optimize infrastructure planning decisions (e.g., charging supply and truck battery size) and time-sequential daily operational decisions (e.g., delivery activities and charging schedules) to achieve a minimum system cost and improve operating efficiency.

3.2 METHODOLOGY

Drayage trucks are utilized for local transportation of cargo and empty containers between shipping terminals and nearby warehouses or distribution centers. The electrification of port drayage trucks entails decision-making at two stages: (a) planning stage: determining the number/type of electric trucks and the number of charging stations to deploy in a port; and (b) operation stage: designing activities of electric trucks during the day to satisfy container throughput requirements. The planning stage decisions on trucks and charging stations will not only influence planning costs, but also determine the availability of trucks and charging stations in the operation stage. At the operation stage, the following decisions are to be made on each operation day:

(1) How many trucks should be assigned to take transport tasks in each period?

(2) Which type of delivery should they make?

(3) When should batteries get charged, considering the electricity price during peak and off-peak hours?

(4) How can trucks avoid unnecessary idling?

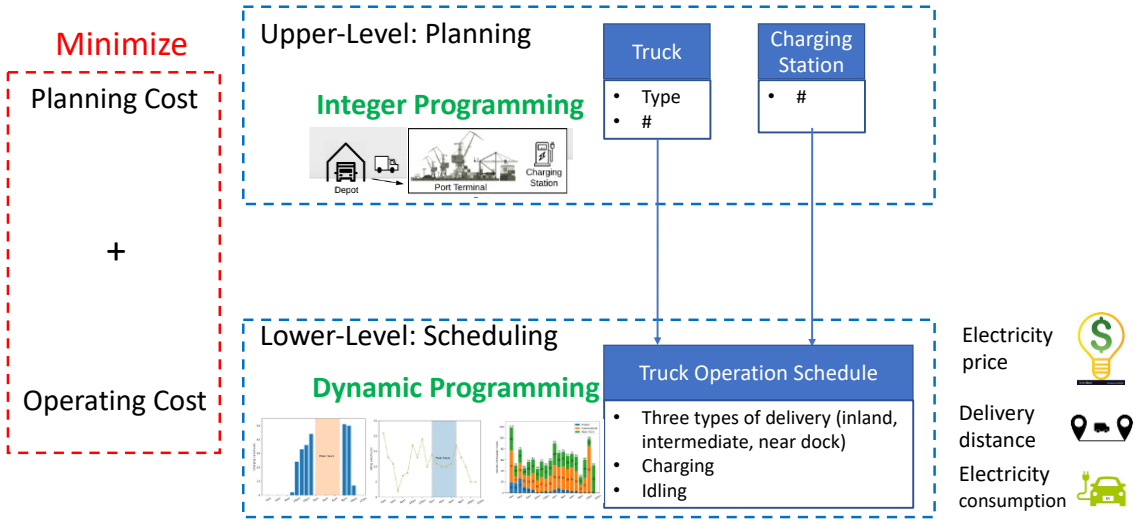

Figure 3.1 Flowchart of concept.

This is a bi-level decision process where the upper level determines resources, and the lower level determines how resources are used. The ultimate objective is to minimize total costs. From a central operator perspective, to find optimal decisions at the upper-level planning stage (number of electric drayage trucks, charging stations) and lower-level operations stage at hourly resolution (scheduling operational activities) while fulfilling container throughput requirements. Specifically, the lower-level operations stage includes a sequential truck activity decision during each scheduling hour. The decision of one truck at one scheduling hour will be influenced by prior decisions of that truck and other trucks (through charging station availability). This sequential decision-making can be solved using a dynamic programming method. The overall objective is to achieve a minimum summation of infrastructure and operating costs.

With the notation defined in Table 3.1, the author can define some functions and then introduce the bilevel optimization model. There are three types of decision variables, i.e., the total number of electric drayage trucks to purchase, y_I, the total number of charging stations to install, y_K, and daily decision $x_{n,i}^a$. $x_{n,i}^a = 1$ is a binary variable, and it equals 1 if truck i is conducting activity a in period n. There are a total of 6 activities, thus, a can

be 1 to 6 each corresponds to different activities as shown in Table 3.1. Dynamic programming algorithm requires definitions of status variables, which include truck battery state of charge (SOC) $S_{n,i}$ and vehicle delivery remaining hour $R_{n,i}$. The transition function of SOC status variable is $S_{n+1,i} = S_{n,i} - \sum_{a=1,2,3} \gamma_i^a \cdot x_{n,i}^a + \gamma_i^4 \cdot x_{n,i}^4$, which subtracts delivery consumption from the previous stage SOC or add charged battery capacity. The transition function for vehicle delivery remaining hour is $R_{n+1,i} = R_{n,i} + \sum_{a=1,2,3} x_{n,i}^a \cdot (h_a - 1) - x_{n,i}^6$. In operational stages, decisions are made in every stage (i.e., one hour), but vehicle delivery can take several hours. Thus $R_{n,i}$ is used to record the number of remaining hours for a truck delivery trip. $R_{n,i}$ equals 0 when truck *i* finishes a delivery trip and back to port at *n*-1 or a truck is not choosing any delivery trip (i.e., $a \neq 1,2,3$).

Table 3.1 Notation and nomenclature.

Parameters	Description
$\boldsymbol{n}$	Index of time stage in the operational decision process, n={1,…,N}
$\boldsymbol{i}$	Index of vehicle, i={1,…., y_I}
$\boldsymbol{a}$	Index of activity decision by vehicles, a={1: long-distance delivery, 2: middle-distance delivery, 3: short-distance delivery, 4: charging, 5: idling, 6: a vehicle is on a delivery trip}
$\boldsymbol{c_I}$	The unit cost associated with the type of truck, $/truck
$\boldsymbol{c_K}$	The unit cost of building an electric charging station, $/station
$\boldsymbol{\beta_n^a}$	a=1, 2, 3: delivery associated cost at stage n, $/hour a=4, 5: labor cost associated with charging or idling at stage n, $/hour
$\boldsymbol{\varepsilon_n}$	Electricity associated cost at stage n (peak/off-peak hours), $/hour
$\boldsymbol{\gamma_i^a}$	a=1, 2, 3: energy consumption associated with deliveries for vehicle i, kWh a=4: battery energy recovery while charging for vehicle i, kWh
$\boldsymbol{h_a}$	a=1, 2, 3: required hours for deliveries, hours
$\boldsymbol{U_i}$	Battery capacity for vehicle i, kWh
$\boldsymbol{L_i}$	Battery minimum level for vehicle i, kWh
$\boldsymbol{T_a}$	a=1, 2, 3: required daily throughput for deliveries, TEUs
Value functions	
$\boldsymbol{\varphi_c(y_I, y_K)}$	$\boldsymbol{\varphi_c(y_I, y_K)} = c_I \cdot y_I + c_K \cdot y_K$ Infrastructure cost for y_I electric trucks and y_K charging stations
$\boldsymbol{\varphi_g(y_I, y_K)}$	$\varphi_g(y_I, y_K) = \sum_{n=1}^{N} \sum_{i=1}^{y_I} \sum_a \beta_n^a \cdot x_{n,i}^a + \sum_{n=1}^{N} \sum_{i=1}^{y_I} \varepsilon_n \cdot x_{n,i}^4 \cdot (S_{n,i} - S_{n-1,i})$ Operational cost when daily throughput is met of y_I electric trucks and y_K charging stations
$\boldsymbol{\varphi_T^a(y_I, y_K)}$	$\varphi_T^a(y_I, y_K) = \sum_{n=1}^{N} \sum_{i=1}^{y_I} x_{n,i}^a, a = 1, 2, 3.$ Operational daily throughputs under y_I electric trucks and y_K charging stations
Decision variables	
$\boldsymbol{y_I}$	Total number of trucks to purchase, including large and small
$\boldsymbol{y_K}$	Total number of electricity chargers to install
$\boldsymbol{x_{n,i}^a}$	Binary variable, whether vehicle i takes activity decision a at stage n
Status variable	
$\boldsymbol{S_n}$	State of charge of all vehicles at stage n, $S_n = \left(S_{n,1}, \dots S_{n,i} \dots, S_{n,y_I}\right)^T$, specifically, $S_{1,i} = U_i$ and $S_{n,i} \in (L_i, U_i), \forall\, i, n$ $S_{n+1,i} = S_{n,i} - \sum_{a=1,2,3} \gamma_i^a \cdot x_{n,i}^a + \gamma_i^4 \cdot x_{n,i}^4, \forall\, i, n$
$\boldsymbol{R_{n,i}}$	The remaining hours that vehicle i is out for delivery, specifically, $R_{1,i} = 0$ $R_{n+1,i} = R_{n,i} + \sum_{a=1,2,3} x_{n,i}^a \cdot (h_a - 1) - x_{n,i}^6, \forall\, i, n$

The objective as shown in Equation (3.1) contains planning costs and the sum of daily operation cost over five years. The planning cost is defined as $\boldsymbol{\varphi_c(y_I, y_K)} = c_I \cdot y_I + c_K \cdot y_K$, i.e., cost of purchasing y_I electric drayage truck and installing y_K charging station. The daily operational cost $\varphi_g(y_I, y_K)$ is compromised by two parts, $\sum_{n=1}^{N}\sum_{i=1}^{y_I}\sum_a \beta_n^a \cdot x_{n,i}^a$, refers to the total operating cost associated with charging, waiting, and delivery activities, and $\sum_{n=1}^{N}\sum_{i=1}^{y_I} \varepsilon_n \cdot x_{n,i}^4 \cdot (S_{n,i} - S_{n-1,i})$, refers to the total charging cost, wherein $(S_{n,i} - S_{n-1,i})$ refers to the change in battery state of charge (SOC) from period $n-1$ to n. The daily container throughput is defined as $\varphi_T^a(y_I, y_K) = \sum_{n=1}^{N}\sum_{i=1}^{y_I} x_{n,i}^a$ which counts containers delivered by all trucks over periods within a day.

$$Minimize\ W = \varphi_c(y_I, y_K) + \varphi_g(y_I, y_K) \tag{3.1}$$

Subject to

$$\varphi_T^a(y_I, y_K) \geq T_a,\ a = 1, 2, 3 \tag{3.2}$$

$$\sum_{a=1}^{6} x_{n,i}^a = 1\ , \forall\ i, n \tag{3.3}$$

$$\sum_{i=1}^{y_I} x_{n,i}^4 \leq y_K, \forall\ n \tag{3.4}$$

$$L_i - \left(S_{n,i} - \gamma_i^a\right) \leq \mathrm{M} \cdot \left(1 - x_{n,i}^a\right), a = 1, 2, 3, \forall\ i, n \tag{3.5}$$

$$S_{n,i} + \gamma_i^4 \cdot x_{n,i}^4 - U_i \leq \mathrm{M} \cdot \left(1 - x_{n,i}^4\right), \forall\ i, n \tag{3.6}$$

Equations (3.2) to (3.6) are constraints. Equation (3.2) ensures the minimum daily container throughput T_a is met. Equation (3.3) ensures that truck i can perform only one activity in any period n. Equation (3.4) guarantees that at any period n, the number of charging trucks does not exceed the available charging stations. Equation (3.5) controls electric trucks' decisions when their battery state of charge is low. It prevents a truck from choosing any type of delivery activity if the completion of delivery will result in a

battery level below the minimum level. Equation (3.6) states the battery level of a truck cannot exceed battery capacity.

For operation cost $\varphi_g(y_I, y_K)$, the decision space is $N \cdot y_I$, wherein *N* is the number of decision periods and y_I is the number of decisions to be made in each period. The computational demand exponentially expands with an increase in the dimensionality of the decision space. A dynamic programming model can significantly reduce the computational power required for solving the model compared with traditional programming models when the problem has inherent characteristics like a dynamic nature (Chen et al., 2017; Wang et al., 2017; Zhang et al., 2018). The author approaches the second stage operating cost minimization problem with a multiperiod dynamic programming model and convert the one-time $N \cdot y_I$ decision space into N sequential period decisions with only y_I decisions to be made in each period. Specifically, the author defines the value function $Z_n(\boldsymbol{S_n})$ as the minimum operational cost from period #1 to #*n* with the state set $\boldsymbol{S_n}$. Therefore, the objective function in operation stage $\varphi_g(y_I, y_K)$ equals $Z_N(\boldsymbol{S_N})$. According to Bellman's principle of optimality (Bellman and Dreyfus, 2015), *n*-stage decision-making can be considered a process of the first *n*-1 stages plus the last n^{th} stage. Thus, the author can define the recursive value function $Z_n(S_n)$ as

$$Z_n(\boldsymbol{S_n}) = \min_{x_{n,i}^a}\left\{Z_{n-1}(\boldsymbol{S_{n-1}}) + \sum_{i=1}^{y_I}\sum_a \beta_n^a \cdot x_{n,i}^a + \sum_{i=1}^{y_I} \varepsilon_n \cdot x_{n,i}^4 \cdot \left(S_{n,i} - S_{n-1,i}\right)\right\} \quad (3.7)$$

The boundary conditions are $Z_0(\boldsymbol{S_0}) = 0$, which means no operating costs are incurred before the operation stage starts, and $S_{0,i} = U_i$, which assumes all trucks start with a fully charged status.

Table 3.2 Summary of input parameters.

Parameter	Value	Reference
Vehicle parameters		
Battery sizes of electric trucks	Truck Type 1: 250 kWh Truck Type 2: 500 kWh	250 kWh (Sen et al., 2017) for regular trucks. 500 kWh (Earl et al., 2018) for high-end trucks.
Cost parameters		
Cost of electric truck	250 kWh: $288,000 500 kWh: $360,000	The study conducted for the ports of Long Beach and Los Angeles (Husing et al., 2007).
Cost of charging station	$105,000 (including installation and materials)	Assuming 200kW direct current fast charging (Husing et al., 2007).
Cost of electricity	$0.28 per kWh (off-peak) $0.56 per kWh (peak)	Los Angeles Department of Water and Power's time-of-use rate plans.
Labor and maintenance costs for the delivery, charging and waiting	Delivery: • Labor: $9.8/hour • Charging and waiting: $4.9/hour	Cost assumptions are consistent with the technical report of electrification for the ports of Los Angeles and Long Beach (Filippo et al., 2019).
Budget period	Five years	Often used for infrastructure ownership and financing analysis (Filippo et al., 2019).
Operation parameters		
Truck operation hours	4 a.m. to 12 a.m.	
Minimum Container throughput	1,299 TEUs/day	5% of total TEU throughput at the POLB and POLA.
Round-trip delivery distance/time/% of TEUs	Near dock: 4mi/1hr / 10% Intermediate: 22mi/2hr/50% Inland: 108mi/4hr/40%	Average distance, time, and percentage of TEUs for three tiers of trips based on a real-world study at ports of Long Beach and Los Angeles (Prohaska et al., 2016).
Round-trip delivery energy consumption (truck type 1 / type 2)	Near dock: 7kWh/10kWh Intermediate: 53 kWh/66kWh Inland: 146kWh/162kWh	Average distance, time, and energy consumption for three tiers of trips based on a real-world study at Port of Long Beach (Prohaska et al., 2016); note the type 2 truck (500 kWh) energy consumption per trip is larger because type 2 trucks are heavier and thus, require more energy for propulsion
Charging station power	150 kW	Assumptions from a technical report of electrification for ports of Los Angeles and Long Beach (Filippo et al., 2019).
Initial truck battery state of charge	100%	All electrics are assumed to be fully charged during the no-activity time of 12 a.m.-4 a.m.

The author implements our proposed model on a case study at the Port of Long Beach (POLB) and Port of Los Angeles (POLA) and builds the model based on empirical input parameters (see Table 3.2). The input for daily port throughput is 1,299 TEU containers, which is 5% of the total containers processed at San Pedro Bay Port Complex (a combination of the POLA and POLB), the largest port in the United States. The author assumes three tiers of delivery trips, with round trip distances of four miles, 22 miles, and 108 miles, respectively. This categorization is based on a study conducted by the National Renewable Energy Laboratory (NREL) (Prohaska et al., 2016) using more than 36,000 miles of in-use drayage truck data collected at the POLA and POLB. The tier #1 drayage truck trip covers most of the port area and near-dock trips, which transfer containers between shipping carriers. The tier #2 trip is referred to as an intermediate trip, which mainly transfers containers to railyard or similar facilities that are relatively close to ports. The tier #3 trip is an inland trip, which transports containers from arriving ships to warehouses at inland locations and delivers containers to final locations using long-haul trucks. The laboratory report provides data such as trip distance, duration, and percentage of twenty-foot equivalent units (TEUs) for each tier of drayage truck trips based on real-world data.

3.3 CASE STUDY AND RESULTS

The author runs the dynamic programming model to solve for optimal planning and operation decisions for the port electric drayage truck optimization that satisfies the 1299 TEUs per day throughput requirement. The composition of TEUs is 129 TEUs (inland), 640 TEUs (intermediate), and 530 TEUs (near-dock), respectively.

Table 3.3 Trucks, charging stations and costs under different scenarios.

Scenarios	#1	#2	#3
# of 500 kWh battery trucks	125	0	60
# of 250 kWh battery trucks	0	140	70
# of chargers	22	51	34
Infrastructure cost	$47 m	$46 m	$45 m
Operation cost	$78 m	$75 m	$75m
Total	$125 m	$120 m	$119 m
Per-TEU cost	$52.9	$50.8	$49.1

The author tried to search for optimal solutions for various scenarios considering different battery-size trucks. The results in Table 3.3 show that, in Scenario#1, there are at least 140 trucks with normal battery sizes (250 kWh) and 51 charging stations needed for daily TEU transport requirements. The infrastructure cost is $45,675,000, and the five-year operating cost reaches $74,692,359, making a total five-year cost of $120,367,359, i.e., $50.8 per TEU. If only considering trucks with large battery sizes (500 kWh, see Scenario#2), it requires 125 trucks and 22 charging stations, with a higher average cost of $52.9 per TEU over a five-year budget period. This is because larger battery-size trucks are heavier and have higher energy consumption rates, which contributes to a higher operation cost. Therefore, to take both advantages of higher endurance mileages from the large batter-size trucks and lower energy consumption rates from the regular ones, Scenario#3 comes to the most economically friendly solution in our case studies with a combination of two types of trucks, 60 large battery-size trucks

and 70 normal battery-size trucks with 34 charging stations, whose average five-year budget cost is only $49.1 per TEU.

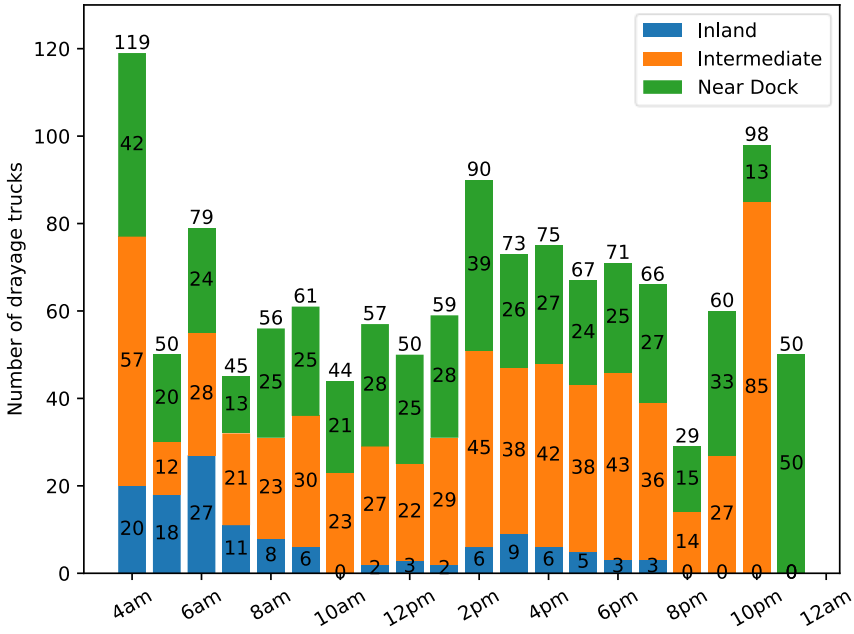

Figure 3.2 The number of deliveries as a function of operating periods.

Apart from minimizing the total cost, the model also provides an optimal daily operating schedule. To make the truck battery sizes consistent in the same fleet, the author only presents optimal operation decisions for the case with 140 normal battery (250 kWh) trucks and 51 charging stations as in Scenario#1. Figure 3.2 summarizes three kinds of delivery decisions made at each stage. Note that it only counts the number of drayage trucks that make delivery decisions right in the current stage. Trucks that are either on a delivery trip or in charging or idling are excluded (the numbers of truck charging and idling activities are reported in Figure 3.3 and Figure 3.4, respectively). For example, if there are 20 trucks determining to make inland deliveries at 4 a.m., then these

trucks will not be repeatedly counted between 5 a.m. to 8 a.m. (an inland round trip takes four hours).

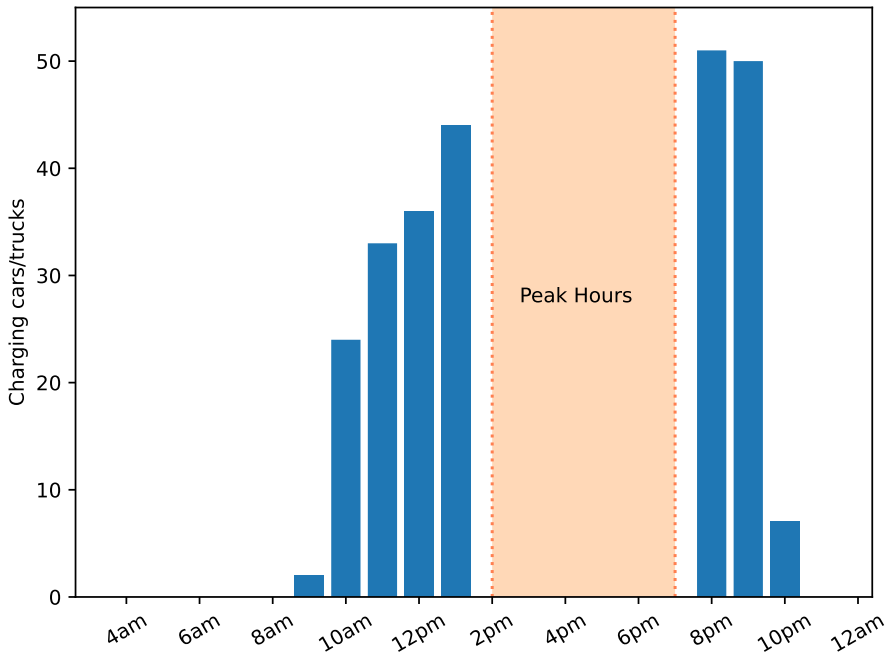

Figure 3.3 The number of charging stations as a function of operating periods.

Figure 3.3 shows the number of trucks that are in charge as a function operation period. It shows that there is no truck choosing to charge during the peak hours, i.e., 2 p.m. to 7 p.m. This is reasonable because the electricity rate during peak hours is twice that in off-peak hours. The optimized results show that an increasing number of trucks tried to be charged before the peak hours and a high-level charging volume can be seen in the first two hours right after the peak hours. In addition, when it comes to the peak hours, it is also interesting to point out that there is a significant increase in the number of trucks to deliver TEU activities at 2 p.m. in Figure 3.2 so that there will be fewer trucks idling at the port during peak hours because of low battery status (see Figure 3.4).

Figure 3.4 shows the number of trucks that are in idle status as a function of time.

Several reasons can lead to an idling decision at each stage. One is that after several deliveries, the truck's battery cannot afford another delivery before getting charged; however, when there are not enough chargers, drivers have no other choice but to wait. Another possible reason is that the model will proactively reserve some trucks idling at the beginning in case that a high charging volume will be encountered when they all return to the port and need charging at the same time. For example, at the beginning of 4 a.m., 21 trucks, accounting for 15% of the total fleet, are purposely assigned idling for the second reason while there is a spike in the number of idling trucks at 7 p.m., and in this case, they are more likely waiting to get charged because the charging stations are limited (see the high-level of charging volumes in Figure 3.3 at 8 p.m. and 9 p.m.).

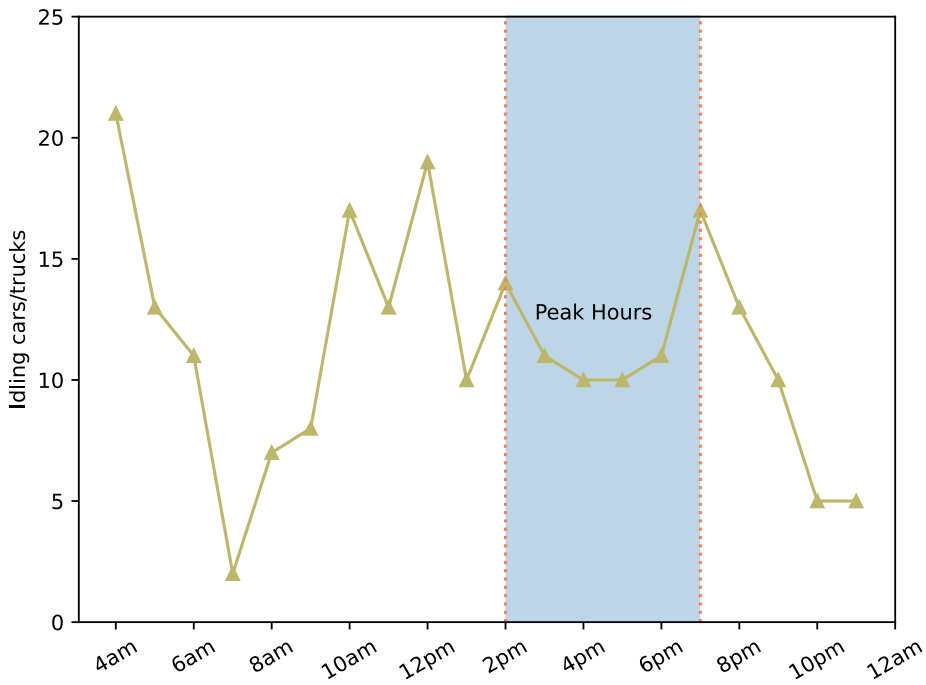

Figure 3.4 The number of trucks in idling status as a function of operating periods.

Table 3.4 presents the time distribution of each activity. Three kinds of deliveries, inland, intermediate, and near-dock deliveries, take up the most time each day, accounting for 83.07%, whereas charging and idling almost equally share the rest of the time, at 8.82% and 8.11%, respectively. This implies that the optimal operation schedule makes the most use of time and truck capacities to accomplish the TEU transport requirements.

Table 3.4 Time distribution of truck activities in a daily operation.

Activity	Throughput	Hours	Time Percentage
Inland delivery	129 TEUs	516 hr	18%
Intermediate delivery	640 TEUs	1,280 hr	46%
Near-dock delivery	530 TEUs	530 hr	19%
Charging	--	247 hr	9%
Idling	--	227 hr	8%
Total	1,299 TEUs	2,800 hr	100%

The author implements the optimization program in a high-performance computing (HPC) cluster available at the University of South Carolina, Hyperion. The author uses one node from the HPC cluster, and each node has 28 cores, with 2.8 GHz computing speed and 128 GB memory, which can perform parallel computing. It takes the computer about five minutes to find the optimal fleet size, charging station and daily activity schedules for a daily throughput of 1299 TEUs, i.e., 50,000 annual TEUs, which is about 5% of the TEUs processed at the largest port in the United States, POLA. The author scales up the computation from 5% of annual TEUs to 10%, 25%, 50% and 100% of POLA's TEUs and reports the corresponding computing time in Figure 3.5.

The author expects the framework can be adopted for real-world applications. If a port is planning to introduce electric drayage trucks, our bilevel model can be used to determine the optimal size and battery composition of the truck fleet and number of chargers, given any level of desired throughput to fulfill with electric trucks. As shown in

Figure 3.5, the annual TEUs of ten million is the throughput currently fulfilled at POLA which is the largest port in the United States. For the whole port to implement drayage electrification, it takes about 180 minutes, or three hours, to determine the planning decisions and corresponding daily operational schedules. The lower-level dynamic programming-based schedule optimization model takes one to two minutes, which enables port authorities to easily modify their daily schedule if there is anything changed in their available charging stations and electric truck.

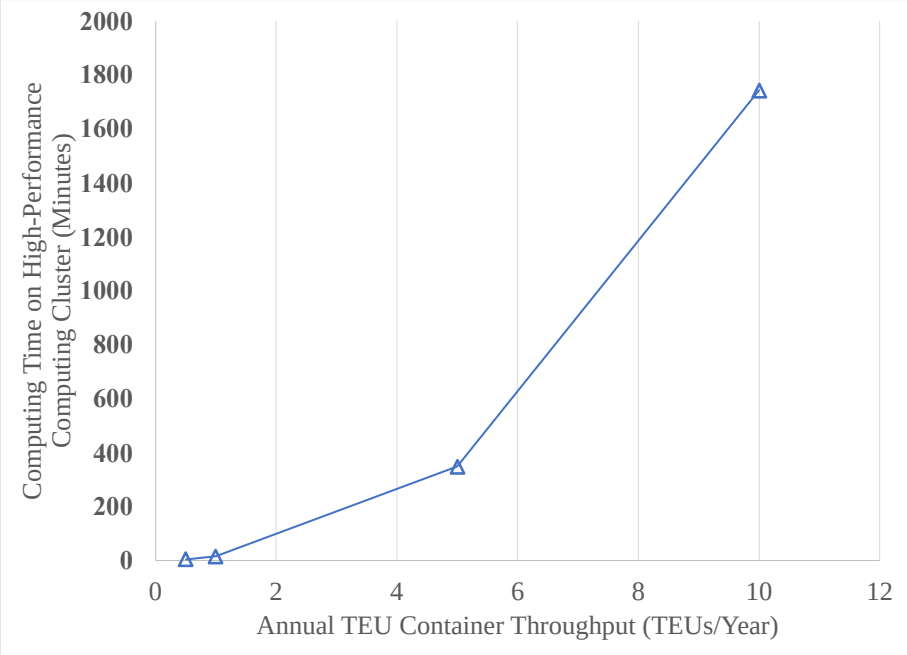

Figure 3.5 Computation time (minutes) on high-performance computing cluster as a function of annual TEU container throughput.

3.4 CONCLUSIONS

In this research, the author proposes a bilevel mixed-integer programming model to co-optimize infrastructure planning decisions (e.g., charging supply and truck battery size) and operational decisions (e.g., delivery activities and charging schedules) to minimize system costs for electrification at ports. The operational stage is a multiperiod decision process in nature, and the author developed a dynamic programming model to

convert a problem with high dimension and computational demand to a sequence of subproblems that have recursive features and much lower solution dimensions.

To demonstrate the applicability of our model, the author implemented a numeric experiment to plan and schedule 5% of daily container throughput at the POLB and POLA, the largest ports in the United States, which can help save GHG emissions, more specifically, 0.62 ton of PM2.5, 112.12 tons of NOx, 0.45 ton of SOx, 38.28 tons of CO and 47,860.22 tons of estimated CO_2 per year (Starcrest Consulting Group, 2022) (estimated from heavy-duty and diesel-fueled trucks with an equivalent 5% amount of TEU transport mileage, i.e., 72,356 mi/day). Assumptions on the battery size of the trucks, the number of charging stations, electricity price, energy consumption rate, and various costs in operations and infrastructure were made based on relevant studies on electric drayage trucks at ports. The proposed model can find the optimal size of the fleet and the number of charging stations to minimize system costs for the desired daily container throughput. In addition, the model generates optimal delivery and charging schedules at one-hour granularity for the truck fleet. Generally, the optimized schedule avoids charging activity in the afternoon hours, the peak electricity price period. The optimized schedule arranges more deliveries (particularly long-distance deliveries) in the early morning and late evening because traffic congestion is the least during those periods. The author also compared scenarios when electric trucks have two different battery sizes, i.e., 500 kWh and 250 kWh. The findings of this paper have implications for electric drayage truck operations in ports. First, it is important to prepare an electric drayage truck fleet based on the daily throughput of the port. The fleet can be optimized for the number of trucks, the number of charging stations, and daily operational schedules. Second, a detailed cost–benefit analysis is needed

to determine the battery size of electric trucks. This analysis should consider various factors, including typical drayage truck trips, traffic conditions in the area, and availability of charging stations at ports. Third, electricity price is an important determinant of the cost of port electrification. The author implements the model with different throughput levels on a high-performance computing cluster and find when annual throughput increases from 50 thousand (5% of LA ports throughput) to ten million (100%), the computation time increases from five minutes to about three hours.

Future research can focus on relaxing some assumptions or constraints developed in this dynamic programming framework to improve its applicability in real scenarios, including (a) increasing the granularity of the modeling period from the current 1 hour to 30 minutes or even 15 minutes so that the operation scheduling is more flexible, and (b) incorporating stochasticity in drayage truck trip distance and energy consumption. And finally, (c) as for social welfare, with the tons of GHG emissions saved from heavy-duty diesel trucks, the public can expect a cleaner and more eco-friendly environment and to live a healthier life at a minimum effect on social economic development.

CHAPTER 4

ELECTRIFYING MIDDLE-MILE TRUCK FLEETS WITH MINIMAL INFRASTRUCTURE REQUIREMENTS[2]

4.1 INTRODUCTION

In 2022, there were 13.8 million new vehicles sold in the United States, with approximately 0.92 million of them being electric("36 Automotive Industry Statistics [2023]," 2023). Vehicle electrification has emerged as a new trend in recent years, with increasing public attention being paid to environmental issues (such as carbon, oxides of nitrogen, and sulfur oxide emissions) related to cargo shipping activities (Chen et al., 2023; Wu et al., 2023). As per the most recent U.S. National Blueprint for Transportation Decarbonization, although medium and heavy-duty vehicles (MHDVs) constitute only 5% of all vehicles on the road, they generate 21% of transportation emissions, making them the second-largest emission contributor after light-duty vehicles (US EPA, 2023b). The electrification of heavy-duty vehicles is deemed a viable strategy for mitigating emissions produced in the transportation sector. This is particularly relevant for the highway freight system. Taking the State of South Carolina (SC) as an example, recent reports indicate that the Port of Charleston in SC has successfully processed approximately 2.4 million TEUs and 1.3 million pier containers in the first half of 2023;

[2] Wu, X., Luo, Q. and Chen, Y., Electrifying Middle-Mile Truck Fleets with Minimal Infrastructure Requirements. To be submitted to a journal.

in the month of May alone, the port handled over 20 thousand vehicles for global automakers

(“SC Ports’ volumes increase across business segments - SC Ports Authority,” 2023). Additionally, the automotive manufacturing, transportation, and warehousing sectors contribute to around 3% of America's GDP and provide approximately 1.25 million job opportunities(“36 Automotive Industry Statistics [2023],” 2023). The embrace of electric vehicles in the automotive industry opens door to new opportunities for suppliers and manufacturers to transform to lean and smart manufacturing.

While earlier studies have predominantly concentrated on developing battery technology for electric heavy-duty vehicles (EHDVs) (Budde-Meiwes et al., 2013; Ma et al., 2021; Manthiram, 2017; Manzetti and Mariasiu, 2015; Soloveichik, 2011; Young et al., 2013), greater emphasis needs to be placed on resolving logistical and operational challenges in highway systems. Specifically, the limited driving range has been a significant barrier for prospective EHDV buyers. According to the U.S. Federal Highway Administration, long-distance trucks travel over 100 thousand miles each year, with drivers expected to cover 430 to 645 miles per day. Since the current estimated driving ranges for EHDVs are from 230 (Freightliner eCascadia) to 350 miles (Nikola Tre Bev) on a full charge (Teran, 2022), expanding the battery capacities or including recharging options become a critical problem. However, delays due to recharging or equipping heavier battery packs will deem a waste of efficiency or resources in the transportation industry that is already under intense pressure to deliver cargo as quickly as possible. More importantly, building new charging infrastructure along highways will necessitate substantial investments and cause new threats to the capability of power grids. These challenges motivate us to develop innovative infrastructure solutions to the widespread deployment of EHDVs.

Compared to traditional strategies that involve recharging at depots or specific charging stations, the battery swapping method offers the advantage of time-saving and becomes a promising solution to alleviate "range anxiety" for EHDVs (Li, 2014; Yang and Sun, 2015). However, there still exist three major concerns on the battery swapping model. The first consideration is that the establishment of new battery swapping stations (BSSs) entails additional infrastructure investments, and these stations will require ongoing maintenance throughout their lifecycle after being put into operation. Secondly, the operational efficiency of the logistic system will heavily depend on the selection of the BSS infrastructure locations. Finally, Once the BSSs are established, they are considered permanent structures and cannot be easily relocated or expanded within a specific timeframe. Consequently, they may not be able to accommodate significant fluctuations when truck routing plans change.

Therefore, in this research, we propose a novel approach to address the EHDV location-and-routing problem, i.e., transporting battery packs to the exchange nodes and replacing the depleted ones from trailers during loading/unloading times. This approach requires minimal effort for establishing new charging infrastructures and allows for easy adaptation to fluctuating demands in the early deployment phase of EHDVs. Figure 4.1

illustrates the concept of the trailer battery exchange strategy adaptation to fluctuating demands in the early deployment phase of EHDVs.

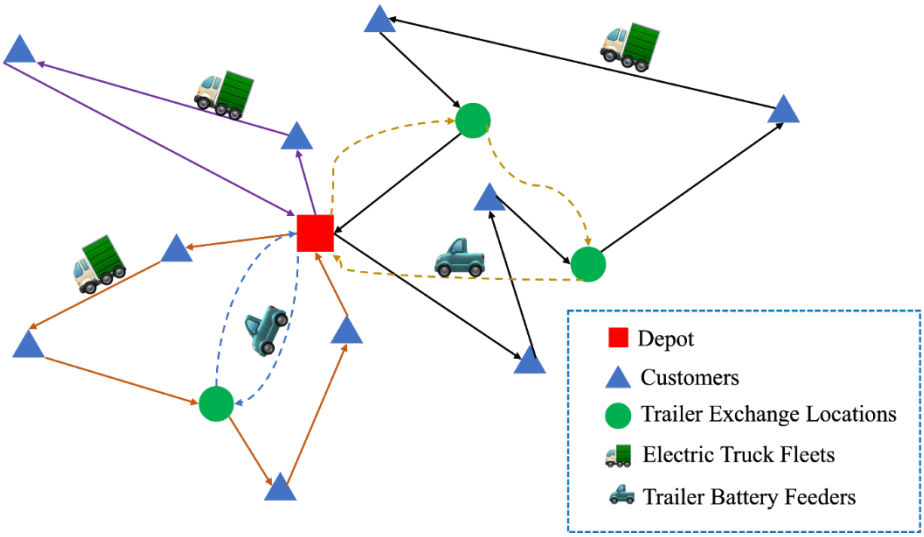

Figure 4.1 Concept of trailer battery exchange strategy.

4.2 METHODOLOGY

In this research, the term "truck" refers to a combination of a tractor and a trailer, which is most common for middle-mile transportation tasks. The author focuses on studying the EHDVs location-and-routing problem (LRP) for the delivery of goods to a set of customers starting from a single depot. The main constraints include routing, battery driving range and payload/capacity constraints. Consider a set of nodes on a graph consisting of a single fixed depot, a group of customers located near the depot, and a set of potential trailer exchange locations. For concision, the author only considers deliveries but not pickups. Each delivery trip starts and ends at the depot and each customer must be visited exactly once by one truck platoon, i.e., multiple visits are not allowed. Each route allows multiple visits to the depot by the same truck for reloading and exchanging trailers. And battery packs of an electric tractor consist of a large-capacity battery, which will not be recharged during the operation period (to save idling time for unpaid workers)

and an exchangeable trailer that equipped with a small-capacity battery pack. Electric trucks have the option to exchange for a fully charged trailer battery pack either at the depot or any of the designated trailer exchange locations. Note that the back-up battery packs required for these exchange locations must be transported from the depot in advance by the feeder vehicle. Therefore, this research does not need to consider the battery exchange station setting up cost, but the battery shipping costs instead.

Table 4.1 Notation and nomenclature.

Sets	
I	Set of Customers, $i \in I$.
J	Set of trailer exchange location candidates, $j \in J$.
K	Set of heavy-duty electric truck fleets, $k \in K$.
T	Set of trips, $t \in T$.
F	Set of trailer battery feeders, $f \in F$
$\{o, o'\}$	Set of the depot and the copy.
V	Set of all nodes, $V = I \cup J \cup \{o, o'\}$.
Decision variables	
y_j	Binary, $y_j = 1$ if candidate j is a trailer exchange station; otherwise, $y_j = 0$.
$x_{i,j}^{k,t}$	Binary, $x_{i,j}^{k,t} = 1$ if vehicle k goes from node i to node j at t^{th} trip; otherwise, $x_{i,j}^{k,t} = 0$.
$w_{i,j}^{f,t}$	Binary, $w_{i,j}^{f,t} = 1$ if trailer battery feeder f goes from node i to node j at t^{th} trip; otherwise, $w_{i,j}^{f,t} = 0$.
Parameters	
d_{ij}	Distance between node i and node j.
t_{ij}	Traveling time form node i to node j at the designated speed.
ρ_1, ρ_2	Unit labor cost per hour for truck and battery feeder drivers, respectively.
M	A large number.
q_i	Customer demand at node i, $\forall i \in I$.
U_k	Total loading capacity of truck fleet k, $\forall k \in K$.
u_{ikt}	The on-vehicle load when vehicle k leaves node i for the t^{th} trip, $\forall k \in K, i \in V, t \in T$.
Q_1, Q_2	The battery driving range for electric trucks and trailers, respectively.
P_{ikt}^1, P_{ikt}^2	The maximum distance that the remaining battery power allows when vehicle k arrives at and leaves node g for the t^{th} trip, respectively, $\forall k \in K, i \in V, t \in T$.
s_k	The number of trucks in fleet k, $\forall k \in K$.

4.2.1 A MATHEMATICAL MODEL

In this section, the author proposes a mathematical model of the problem. To get started, notations that will be used in this paper are listed in Table 4.1.

Now the electric vehicle routing problem can be formulated as follows:

$$\min \sum_{i\in V}\sum_{j\in V}\sum_{k\in K}\sum_{t\in T}\rho_1\, s_k t_{ij}\, x_{i,j}^{k,t} + \sum_{i\in J\cup\{o\}}\sum_{j\in J\cup\{o'\}}\sum_{f\in F}\sum_{t\in T}\rho_2\, t_{ij}\, w_{i,j}^{f,t} \quad (4.1)$$

Subject to

(For trucks)

$$\sum_{i\in V, i\neq j}\sum_{k\in K}\sum_{t\in T} x_{i,j}^{k,t} = 1\,, \forall j \in I \quad (4.2)$$

$$\sum_{i\in V\setminus\{o,j\}}\sum_{k\in K}\sum_{t\in T} x_{i,j}^{k,t} \leq M y_j, \forall j \in J \quad (4.3)$$

$$\sum_{j\in V\setminus\{o,i\}} x_{i,j}^{k,t} = \sum_{j\in V\setminus\{o',i\}} x_{j,i}^{k,t}\,, \forall i \in V\setminus\{o,o'\}, k \in K, t \in T \quad (4.4)$$

$$\sum_{j\in V\setminus\{o\}} x_{o,j}^{k,t} = \sum_{i\in V\setminus\{o'\}} x_{i,o'}^{k,t}\,, \forall k \in K, t \in T \quad (4.5)$$

$$\sum_{j\in V\setminus\{o\}} x_{o,j}^{k,t} \leq 1, \forall k \in K, t \in T \quad (4.6)$$

$$u_{jkt} \leq u_{ikt} - q_j x_{i,j}^{k,t} + U_k\left(1 - x_{i,j}^{k,t}\right), \forall i \in V\setminus\{o'\}, j \in V\setminus\{o\}, i \neq j, k \in K, t \in T \quad (4.7)$$

$$u_{okt} \leq U_k, \forall k \in K, t \in T \quad (4.8)$$

$$u_{jkt} \geq 0, \forall j \in V\setminus\{o'\}, k \in K, t \in T \quad (4.9)$$

$$P_{jkt}^1 \leq P_{ikt}^2 - d_{ij} x_{i,j}^{k,t} + (Q_1 + Q_2)\left(1 - x_{i,j}^{k,t}\right), \forall i \in V\setminus\{o'\}, j \in V\setminus\{o\}, i \neq j, k \in K, t \in T \quad (4.10)$$

$$P_{o,k,t=1}^2 = Q_1 + Q_2, \forall k \in K \quad (4.11)$$

$$P_{o,k,t\neq 1}^2 = Q_2, \forall k \in K, t \in T \quad (4.12)$$

$$P_{i,k,t}^2 = P_{i,k,t}^1 + y_i\left(Q_2 - P_{i,k,t}^1\right), \forall i \in J, k \in K, t \in T \quad (4.13)$$

$$P^2_{i,k,t} = P^1_{i,k,t}, \forall i \in V \backslash J, k \in K, t \in T \tag{4.14}$$

$$P^1_{ikt}, P^2_{ikt} \geq 0, \forall i \in V, k \in K, t \in T \tag{4.15}$$

$$y_n, x^{k,t}_{i,j} \in \{0,1\}, \forall n \in J, i \in V \backslash \{o'\}, j \in V \backslash \{o\}, k \in K, t \in T \tag{4.16}$$

(For Trailer Battery Feeders)

$$\sum_{j \in J \cup \{o'\} \backslash \{i\}} w^{f,t}_{i,j} = \sum_{j \in J \cup \{o\} \backslash \{i\}} w^{f,t}_{j,i}, \forall i \in J, f \in F, t \in T \tag{4.17}$$

$$\sum_{j \in J \cup \{o'\}} w^{f,t}_{o,j} = \sum_{i \in J \cup \{o\}} w^{f,t}_{i,o'}, \forall f \in F, t \in T \tag{4.18}$$

$$\sum_{j \in J \cup \{o'\}} w^{f,t}_{o,j} \leq 1, \forall f \in F, t \in T \tag{4.19}$$

$$M \cdot \sum_{j \in J \cup \{o'\}} w^{f,t}_{o,j} \geq \sum_{i \in J \cup \{o\}} \sum_{j \in J \cup \{o'\}} \sum_{t \in T} w^{f,t}_{i,j}, \forall f \in F, t \in T \tag{4.20}$$

$$\sum_{i \in J \cup \{o\} \backslash \{j\}} \sum_{f \in F} w^{f,t}_{i,j} \geq \sum_{i \in V, i \neq j} \sum_{k \in K} x^{k,t}_{i,j}, \forall j \in J, t \in T \tag{4.21}$$

$$w^{f,t}_{i,j} \in \{0,1\}, \forall i \in J \cup \{o\}, j \in J \cup \{o'\}, f \in F, t \in T \tag{4.22}$$

The objective (4.1) minimizes total shipping cost, including the shipping cost of trucks and trailer battery feeders. Constraint (4.2) ensures that each customer node will be visited exactly once by one truck fleet. Constraint (4.3) guarantees can only exchange their trailer battery packs at a located exchange node. Constraints (4.4) - (4.6) are flow conservation constraints. Constraint (4.4) guarantees that when a truck visits a node, it must leave the node to the next one. Constraint (4.5) makes sure that a truck starts and ends at the depot. Constraint (4.6) demonstrates that only one trip at most is allowed for each departure from the depot. Constraints (4.7) - (4.9) are related to truck load capacities. Constraint (4.7) is tracking and updating the remaining loaded goods on each truck along its routes. Constraint (4.8) indicates that the initial load at the depot will not exceed truck's payload capacity. Constraint (4.9) makes it clear that the remaining load on trucks must be nonnegative. Equations (4.10) - (4.15) are driving range constraints. Constraint (4.10) is

tracking and updating the remaining battery range for trucks. Constraints (4.11) and (4.12) initialize the maximum battery range for each trip when trucks depart from the depot. Constraint (4.13) shows the trailer battery exchange at located nodes. Constraint (4.14) ensures that the remaining driving range remains at non-exchange nodes. Equation (4.15) is the nonnegative constraint on battery driving range. Equation (4.16) defines the binary truck routing decision variables. Constraints (4.17) - (4.19) are flow conservation constraints for trailer battery feeders. Constraint (4.20) eliminates sub-circle tours among trailer battery feeder routes. Constraint (4.21) indicates that trailer battery feeder must meet the battery exchange demands at a trailer exchange location. Equation (4.22) defines trailer battery feeder routing decision variables as binary variables.

Additionally, if we set the hourly labor cost $\rho_1 = \rho_2 = 1$ in the objective function, then the objective value is also equivalent to the total work hours for both electric trucks and trailer battery feeders.

4.2.2 ALGORITHM

This section gives a brief description of a hybrid method to solve the electric truck routing problem. In the hybrid algorithm, Tabu Search (TS) is employed to search the trailer exchange location strategies and a Mixed Integer Programming (MIP) solver is to decide the optimal routes for both electric trucks and trailer battery feeders.

a. Initialization (Radius Covering)

An initial trailer exchange location solution is basically needed for the problem solving and Tabu Search process. In this paper, we use a radius covering algorithm in (Yang and Sun, 2015) to initialize the set of trailer exchange locations.

Step 1.1: Create an empty customer covering lists (CCLs) for the trailer exchange locations to cover customers who can be reached within a certain serving range $r_c Q$, where $0 < r_c \leq 1$ and Q is the maximum battery driving range.

Step 1.2: A set of trailer exchange locations will be randomly generated and customers within the radius will be automatically added into the corresponding CCL of the candidate location; if there exist any uncovered customers, the trailer exchange location with the minimum number of covered customers will be iteratively relocated until all the customers are covered at least once.

Step 1.3: Return the final set of trailer exchange locations as the initial candidates' solution s_0 and solve the MIP model to obtain the initial objective value v_0.

b. Location Problem (TS process)

The TS process helps to find the optimal set of trailer exchange locations with lower objective values. The results obtained from Tabu Search will work as the input of candidate trailer exchange locations (y_j) to the MIP model.

Step 2.1 (Initialization): For a given number of located trailer exchange locations, obtained candidates' solution and objective value are s_0 and v_0, respectively. Initialize the current solution $s \leftarrow s_0$, current best-known solution $s^* \leftarrow s_0$ and best-known objective value $v^* \leftarrow v_0$.

Step 2.2: (Neighborhood Search) Let J_{loc} be the set of located trailer exchange locations and $J_{un} = V \backslash J_{loc}$ be the unlocated nodes set under the current solution s. TS starts with an empty tabu list, and we exchange one located candidate trailer exchange location in J_{loc} with an unlocated node in J_{un}.

Step 2.3 (Routing Optimization): For each newly generated neighborhood candidate set of trailer exchange locations, solve the MIP model to obtain the corresponding routes and objective values.

Step 2.4 (Solution Updating): Update the current solution $s = argmin(v_s)$, where s is not in the tabu list. However, if the objective value of a neighboring solution is better than the current best-known value, the tabu rule will be violated, i.e., if $v_s < v^*$, then $s^* \leftarrow s_s$ and $v^* \leftarrow v_s$, and update the tabu list accordingly. If the size of tabu list reaches its capacity, then release the first element in the list.

Step 2.5: (Final Solution): If a given number of iterations has been reached, stop searching and report the best-known solution and objective value as the optimized results; otherwise, go back to Step 2.2.

4.3 COMPUTATIONAL EXPERIMENTS

This section presents computational experiments using the FAF data from several Southeast states of the US. The original dataset provides information on U.S. freight Origin-Destination (OD) annual demands by truck tonnages, with 132 FAF zones (Sun, 2020). For our study, we consider Atlanta, GA as the single depot in the southeast network, responsible for transporting goods to destinations in neighboring states based on demand requests (refer to Figure 4.2).

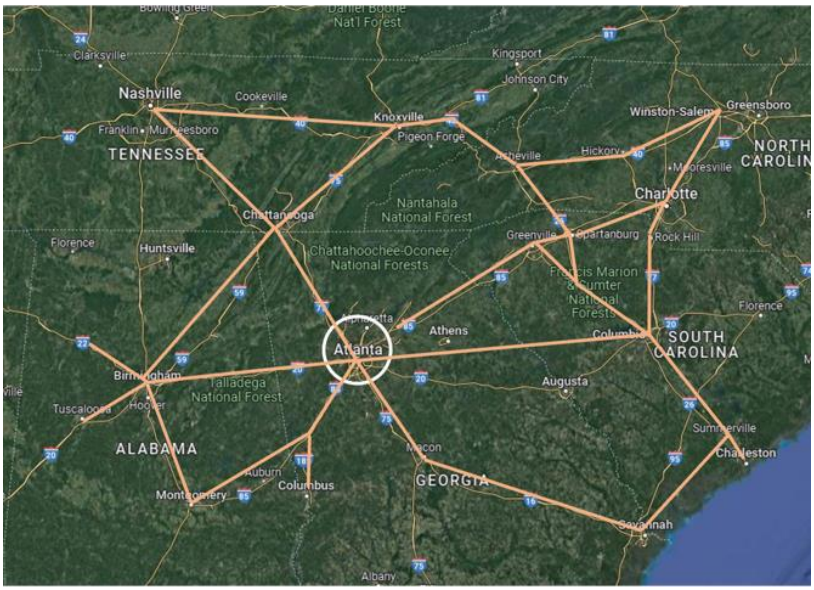

Figure 4.2 Network with the depot at Atlanta, GA.
(Shown in Google Maps)

Based on the results of a series of preliminary experiments, the parameter settings are as follows. Statistically, there are a total of 31 nodes (including the depot) being involved in the studied area. 19 of them are customer nodes, requiring a total of 4,181 tons of goods to be transported from the depot daily. All nodes except the depot can be a trailer exchange candidate location. In the case that a trailer exchange location is just the same node where a customer is, we will manually add a trailer exchange dummy node there, whose distance to the corresponding customer node is zero (Yang and Sun, 2015). The node and location information can be found in Table 4.2 and customer demands are listed in Table 4.3.

Table 4.2 Nodes and locations.

Depot ID: 103			Depot Location: Atlanta, GA		
ID	Location	ID	Location	ID	Location
5	Jasper, AL*	337	Savannah, GA*	382	Tuscaloosa, AL*
6	Birmingham, AL	339	Winston-Salem, NC	412	Summerville, SC
101	Montgomery, AL*	340	Charlotte, NC*	420	Marietta, GA
102	LaGrange, GA*	341	Rock Hill, SC*	421	Adairsville, GA*
243	Buford, GA	342	Columbia, SC	422	Lenoir City, TN
244	Gainesville, GA*	360	Greenville, SC*	435	Ashville, NC
245	Carnesville, GA	361	Clinton, SC	456	Spartanburg, SC*
280	Macon, GA	372	Nashville, TN*	466	Knoxville, TN*
325	Columbus, GA*	373	Murfreesboro, TN*	507	Charleston, SC*
336	Dublin, GA*	374	Chattanooga, TN*	542	Hickory, NC*

Note: Nodes marked with "*" represent customer nodes.

Table 4.3 Customer demands.

ID	Demands/ton	ID	Demands/ton
5	79	372	183
101	377	373	40
102	90	374	40
244	662	382	27
325	744	421	264
336	46	456	140
337	577	466	15
340	189	507	79
341	17	542	3
360	609		
	Sum		4,181

In this initial instance, the battery pack of an electric truck consists of a one-time 350-mile tractor battery and a 300-mile trailer battery to simulate the state-of-the-art electric truck technologies, which will be relaxed in sensitivity analyses. Recall that the tractor battery cannot get recharged (for time-saving considerations) when it runs out and the trailer battery can be exchanged for a fully charged new one within minutes either at a located trailer exchange location or at the depot. The maximum payload capacity of an

electric truck is limited to 20 tons while the customer demands range from three to 744 tons (see Table 4.3), so the author need to organize these electric trucks into platoons or fleets of trucks with identical routes to ensure that there is at least one platoon capable of transporting the goods to customer nodes with high demands.

In the TS process, the author sets the maximum candidate number of trailer exchange locations to six per iteration, the maximum length of Tabu list to five, and the maximum number of TS iterations is determined to be 20.

In our implementations, the author employes a total of 142 electric trucks and assigns them into eight platoons. And for statistical purposes, the author sets the hourly labor cost $\rho_1 = \rho_2 = 1$ in the objective function. Therefore, Figure 4.3 displays the least-known total work hours for both electric trucks and trailer battery feeders. As shown in the figure, the total work hours have dropped from 1,658 hours to 1,618 hours, resulting in approximately 2.4% savings compared to the initial solution. Based on the declining trend of the objective values observed during each iteration of the TS, it can be apparently concluded that an optimized set of trailer exchange location candidates can help effectively reduce the total work hours, and therefore helps to reduce the total operational cost.

To minimize the work hours, TS identifies the definitive set of candidate locations for trailer battery exchange: {6, 101, 337, 342, 421}, with a minimal objective function value of 1,618 hours as shown in Figure 4.3. The electric vehicle routing and trailer battery feeder routing details are provided in Table 4.4.

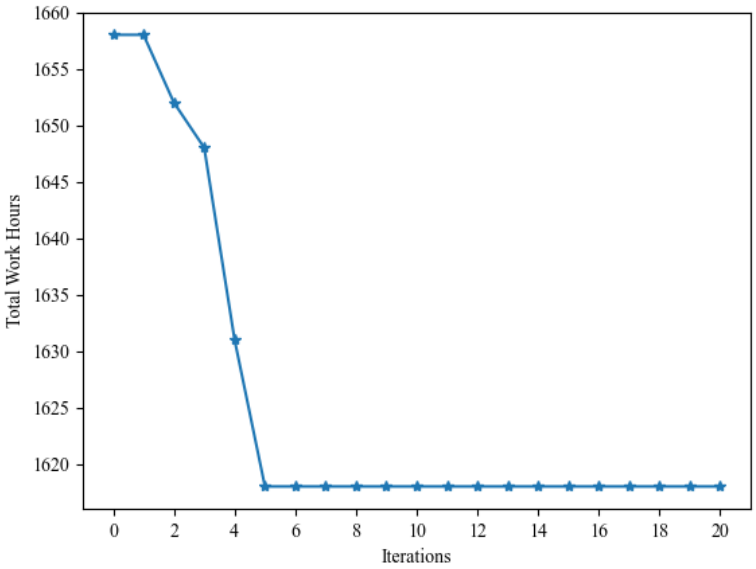

Figure 4.3 TS for optimal trailer exchange locations.

Table 4.4 Optimized routes for electric trucks and trailer battery feeders.

Vehicles	Sizes/trucks	(Loads | Capacity)/ton	Routes
Platoon #1	40	744 |800	Depot-325*-102-Depot
Platoon #1	40	624 | 800	Depot-456*-360*-245-243-Depot
Platoon #2	35	662 | 700	Depot-244*-243-Depot
Platoon #2	35	623 | 700	Depot-336*-337*-280-Depot
Platoon #3	30	527 | 600	Depot-372*-373*-374*-421*-420-Depot
Platoon #4	20	377 | 400	Depot-101*-102-Depot
Platoon #5	10	189 | 200	Depot-340*-341-342-Depot
Platoon #5	10	106 | 200	Depot-382*-6-5*-(6)-Depot
Platoon #6	5	79 | 100	Depot-507*-412-342-Depot
Platoon #6	5	90 | 100	Depot-102*-Depot
Platoon #7	1	18 | 20	Depot-542*-435-466*-422-374-(421)-420-Depot
Platoon #8	1	17 | 20	Depot-341*-342-Depot
Feeder	1	11 battery packs	Depot-421-6-Depot

Note: Nodes marked with "*" represent customer nodes, and nodes marked with brackets indicate exchanging trailer batteries at the corresponding locations.

It becomes clear that the principle of "more is better" does not necessarily apply to the selection of trailer battery exchange locations. Referring to the results obtained in Figure 4.3 and Table 4.4, while there are five potential locations {6, 101, 337, 342, 421} for trailer battery exchanges, only two, namely #6 and #421, have ultimately been chosen as the designated sites. This conclusion is sensible because selecting more trailer exchange locations than necessary would result in additional exchange location setup costs and trailer battery feeders shipping costs for delivering batteries. The results also demonstrate the effectiveness of our optimization model and algorithm.

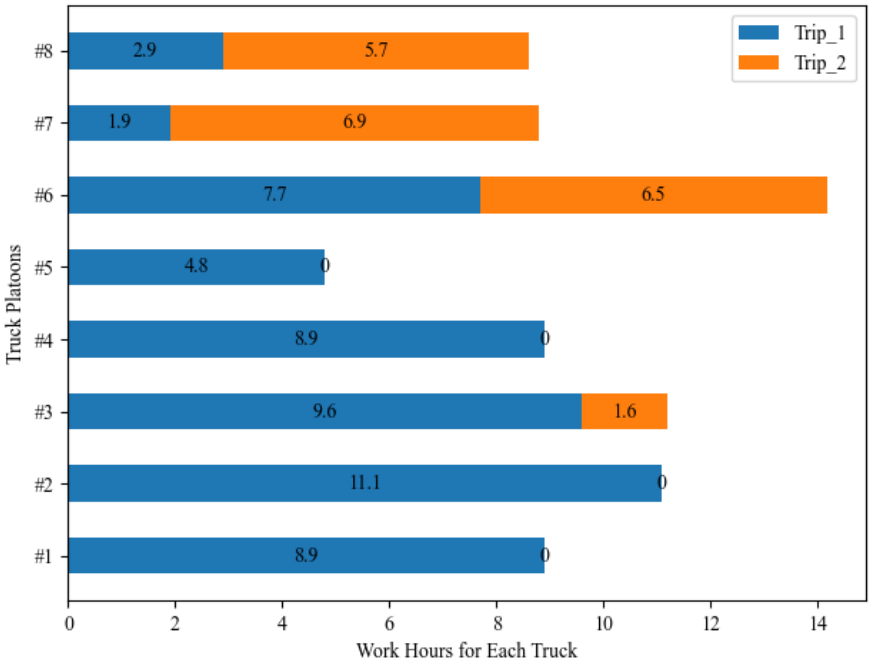

Figure 4.4 Operational schedules for trucks in each platoon.

Figure 4.4 provides a detailed breakdown of work hours for each truck in every platoon. Due to work hour limitations, each truck can handle a maximum of two deliveries per day in our experiments. It is crucial to note that Figure 4.4 exclusively represents the work hours for each truck platoon and does not factor in time allocated for loading/unloading, driver rest periods, or trailer battery exchanges. Furthermore, the results

displayed in Figure 4.4 are not interchangeable. For example, reassigning Trip #2 of truck platoon #6 to platoon #5 is not possible since the truck fleet sizes differ among various platoons. Such reassignments could result in either load capacity constraints violations or the addition of unnecessary system costs.

Yang and Sun proposed a battery swapping strategy for Electric Vehicles (EVs) in their study (Yang and Sun, 2015). In their model, EVs can swap batteries at designated BSSs. The objective function includes both a one-time setup cost for the BSSs and the routing costs for the EVs, while the trailer feeder routing costs do not need to be taken into account. To compare the economic efficiency with the solution of establishing BSSs in (Yang and Sun, 2015), we conduct sensitivity analysis through adding unit shipping cost and station setup cost to the objective functions. Figure 4.5 illustrates the thresholds where the total cost of using trailer exchange surpasses that of establishing BSSs. To achieve this, we first convert the one-time BSS setup cost into an average daily cost based on their budget periods. Then, the author applies the objective function in (Yang and Sun, 2015) to the same network in this research to estimate the total system cost. Consequently, the author

compares the system costs of the two methods under different fare rates and present the comparison results in Figure 4.5.

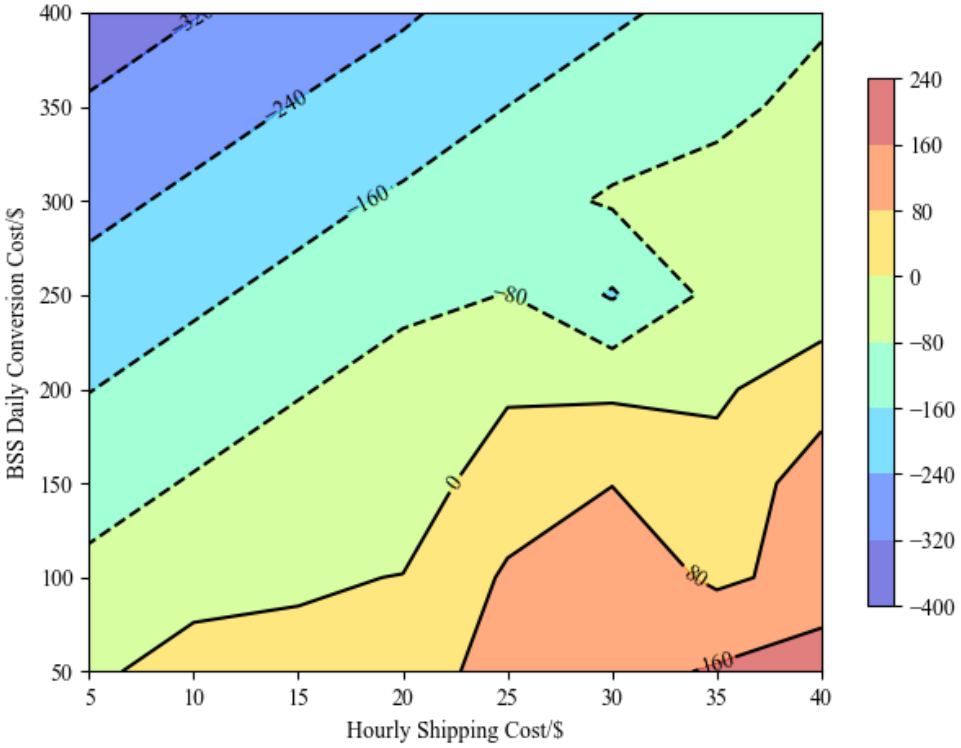

Figure 4.5 Economic comparison of establishing BSSs V.S. trailer exchanging.

For the economic analysis, the conditional boundary is depicted in Figure 4.5 as the contour line with a value of zero. As demonstrated in Figure 4.5, it becomes evident that, in the majority of cases, the trailer exchanging approach proves to be more cost-effective compared to the BSSs strategy. However, in some certain scenarios where the budget period is sufficiently long (observed in the lower right section of Figure 4.5), the average daily conversion cost for BSSs can potentially fall below that of trailer battery exchanging.

Given the adaptability and resilience of the trailer exchanging method, particularly within scenarios characterized by fluctuating customer demands, it can flexibly accommodate real-world requirements with minor adjustments, like relocating trailer

battery exchange locations. This inherent ability to respond to dynamic situations positions trailer exchanging as a favorable and viable choice.

4.4 CONCLUSIONS

Driving range concerns are among the primary limitations on the future adoption of middle mile or long-haul electric vehicles. For many logistics companies, the transition to electric ground freight must condition on establishing reliable and accessible supporting infrastructure to address this issue. In contrast to previous research focused on setting up new charging stations or battery-swapping stations and optimizing their locations along highways, this research presents a more cost-efficient and minimal infrastructure solution: trailer battery exchanging directly at any exchange locations. This electric trailer exchange process can be carried out concurrently while the truck is loading at the depot, loading or unloading at a customer node, or even during the driver's rest at a designated rest area.

In this research, the author presents a mathematical model for the electric truck location-and-routing problem, incorporating a trailer battery exchange strategy, which consists of two interrelated levels of problems. The upper level involves a facility location problem, where the author selects a candidate set of trailer exchange locations. The lower-level deals with the vehicle routing problem given a specific set of exchange locations. To solve the model, the author proposes a hybrid algorithm that combines TS to optimize the trailer exchange locations in the upper level and an MIP solver to address the lower-level mixed-fleet vehicle routing problem. The trailer battery exchange approach proves to be more flexible and economical in most cases compared to the BSS design. The results also demonstrate that implementing the proposed method significantly saves operational costs

due to recharging and payment issues for idling times while mitigating range anxiety with flexible dispatching of feeder vehicles.

However, there are still some real-world implementation limitations in this research. Firstly, like most VRP models in the literature, the author has not considered the impact of load on battery consumption, which will introduce nonlinearity into the problem. Instead, the arc-based energy consumption estimate is solely based on the average traveling distance. Second, the author requires electric trucks within the same platoon to share the same routes to speed up computations, which might not be fully practical in real-world situations. Finally, the total work hours of different platoons have not been adequately balanced, which could potentially lead to fairness issues when scheduling personnels.

CHAPTER 5

INTEHRATING RAILROAD CROSSING BLOCKAGE INFORMATION IN LAST MILE DELIVERY[3]

5.1 INTRODUCTION

The demand for urban freight transportation has significantly increased in recent years due to urbanization, demographic growth, and the widespread adoption of e-commerce platforms like Amazon, Walmart, eBay, and others. Providing logistics services at the right time, from the right location, to the right users, and at a reasonable cost is of significant importance for supply chains. (Juhász and Bányai, 2018). This surge in demand has necessitated an increase in the number of vehicles used for "last mile delivery", ensuring just-in-time delivery of goods to customers (Patella et al., 2021).

To guarantee punctuality in last mile delivery, one way is to optimize the delivery schedule and route. There have been numerous studies on shortest path problems in Chapter 2, however, none of them have taken train blockages into account when determining the shortest path, whether distance-based or time-based. A grade crossing is where a railway and a road cross at the same level. There are approximately 212,000 highway-rail grade crossings across the United States at the end of 2022 (https://railroads.dot.gov/). For a

[3] Wu, X., Qian, Y., Chen, Y., Integrating Railroad Crossing Blockage Information in First Responder Dispatching Route Planning. To be submitted to a journal.

protected grade crossing, gate arms will block the road from an approaching train is detected until the train leaves that track segment. Depending on the train length and speed, the grade crossing blockage time varies a lot, ranging from dozens of seconds in case of only a locomotive quickly passing by for several hours in case of a stopped train at the grade crossing. During the crossing blockage, it is impossible and illegal for any vehicle or person to pass through the blocked track. They have to must yield to approaching or passing trains at the grade crossings until the crossing is cleared, which can take minutes to hours.

Train-blocked grade crossings have significantly disrupted people's daily lives. Federal Railroad Administration (FRA) reported a stopped or slowly moving train blocking a grade might impede the movement of emergency response vehicles (FRA, 2006). In 2015, the FRA acknowledged that complaints regarding blocked crossings ranked as the most common type of complaint they received (Njus, 2016). The travel delay caused by highway-railway grade crossings may account for this phenomenon, especially in North America (Park et al., 2016). These disruptions can inconvenience commuters, reduce punctuality, and adversely affect overall transportation efficiency. For example, Police Chief Mark Veirg in Cokeville, Wyoming, reported the train sometimes sat at the crossing for hours, rendering it difficult for them to decide between waiting and taking a 44-mile detour to turn around (Poe, 2018).

With the conflicts between trains and road traffic becoming more serious, many governments or transportation departments are trying to address the problem. A radar vehicle detection system has been employed for a four-quadrant gate system and blocked crossing (Hilleary and ByStep, 2012). Unforeseen delays at grade crossings frequently pose challenges for delivery vehicles, leading to traffic congestion and hindering postmen from

following their pre-planned routes and meeting their delivery schedules. Unfortunately, there is no system available to share the real-time grade crossing train information and provide situational assessment information to logistical companies and the other involved parties, which raises significant package delivery delays.

Recognizing the substantial impact of blocked grade crossings, this research aims to establish a framework that mitigates such disruptions and enhances the effectiveness of last mile delivery routing planning in these scenarios. Compared to the advanced navigation technologies like Google Maps, the framework in this paper can efficiently dispatch last mile delivery vehicles along routes that minimize travel time and ensure they are not impeded by passing trains.

5.2 METHODOLOGY

This research aims to propose a novel framework for last mile delivery that incorporates potential train blockages. The framework involves several key steps. Firstly, the author identifies grade crossings by comparing the road and railroad networks. Next, using train GPS data, the author estimates the train blockage window at each grade crossing along the train trajectory. Finally, the author employes a modified label correcting algorithm to search for a time-dependent shortest path, ensuring that customers will be visited with the minimum delay caused by passing trains. The layout of the new dispatching framework has been displayed in Figure 5.1.

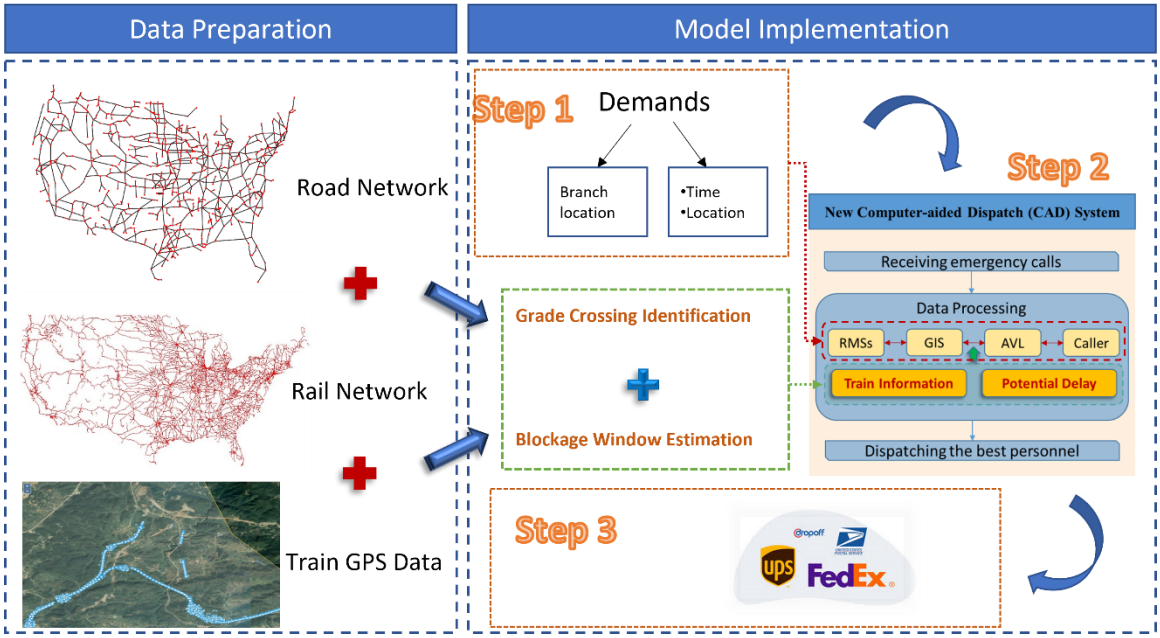

Figure 5.1 Layout of the system framework.

5.2.1 DATA PREPARATION

In this study, we utilized real-world freight train operational data shared by CSX Transportation, Inc. (CSX) at a second-level granularity. The GPS contains detailed information such as time stamps, train IDs, locomotive IDs, locomotive location coordinates, locomotive instantaneous velocity, and train length. The data collects trains operating within a 20 km radius of the City of Columbia, South Carolina, USA, from October 31, 2020, to November 10, 2020. The utilization of this real-world operational data allowed us to conduct an in-depth analysis and develop a comprehensive framework for addressing the issue of train blockages and their impact on last mile deliveries.

Statistically, there is a total of 116 unique train IDs being observed from 39,773 GPS records. By plotting the train trajectories using ArcGIS Pro, we identify six major train route patterns, as shown in Figure 5.2. The proportions of each pattern are (a) 12.1%, (b) 12.9%, (c) 3.4%, (d) 39.7%, (e) 5.2% and (f) 25.9%, respectively. However,

due to security concerns, we are unable to disclose specific train IDs and their corresponding routes.

Figure 5.2 sheds light on how the trains will go through the City of Columbia so that we can predict the train direction for the following minutes. Given current train length, location, and speed information, we can primarily estimate blocked nodes with corresponding blockage windows.

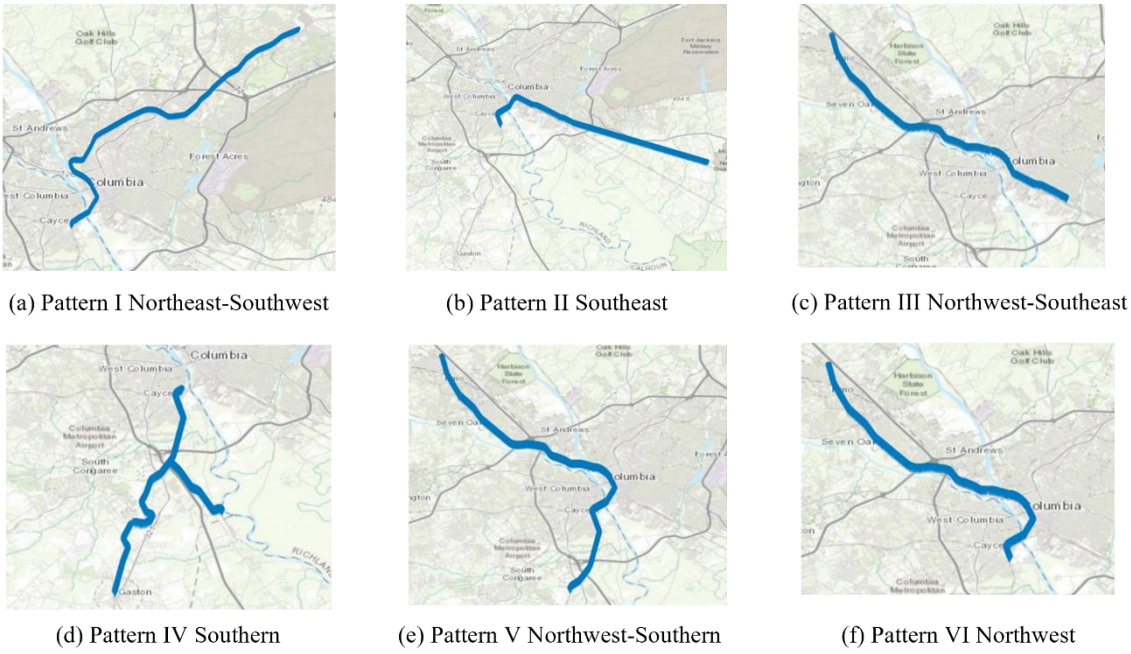

(a) Pattern I Northeast-Southwest (b) Pattern II Southeast (c) Pattern III Northwest-Southeast

(d) Pattern IV Southern (e) Pattern V Northwest-Southern (f) Pattern VI Northwest

Figure 5.2 Major patterns of CSX freight train routes in Columbia, SC (1:242,000 shown in ArcGIS Pro).

Table 5.1 Descriptive statistics of train length from GPS data.

Index	Value
Count	39,773
Mean	1743 m
Standard Deviation	3,773.15
Min	12 m
25 % Quantiles	914 m
Median	1,660 m
75 % Quantiles	2,750 m
Max	5,190 m

Table 5.1 summarizes the length distribution of 39,773 train records. From Table 5.1, it can be seen that the length of trains ranges from 12 to 5,190 meters. Combined with the information on train operating speed (Figure 5.3), readers can briefly infer that the length of train blockage windows might fluctuate from seconds to hours.

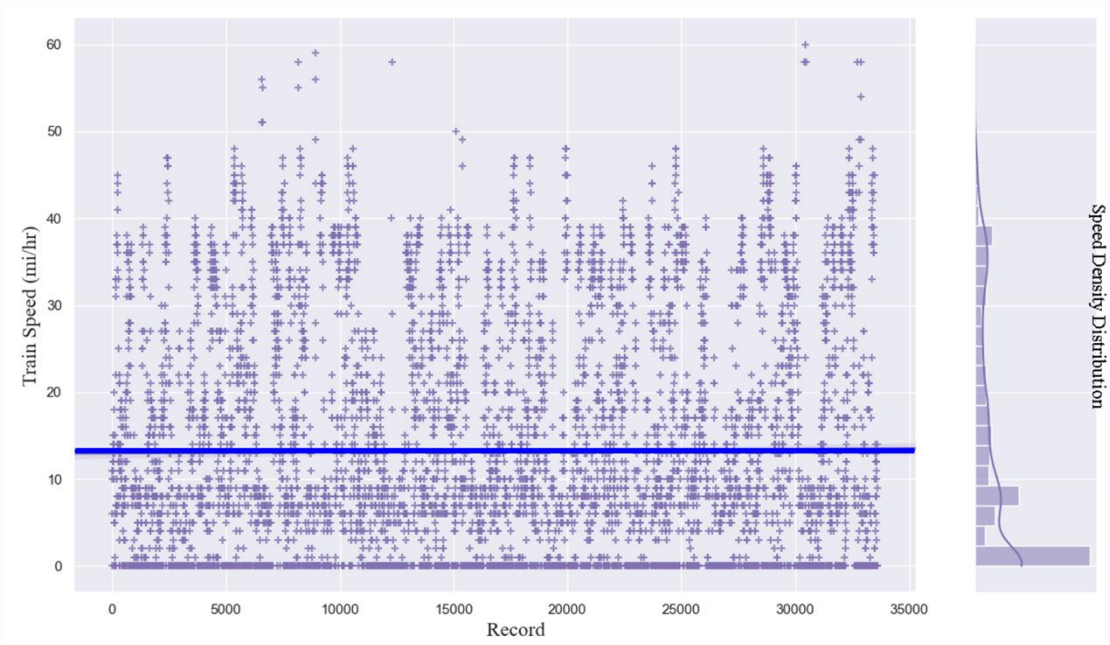

Figure 5.3 Instantaneous train speed distribution from the GPS data.

Figure 5.3 shows the instantaneous velocity distribution of 33,617 trains from the GPS data within 20 km of the City of Columbia center. Figure 5.3 illustrates that train speeds vary from 0 to 96.56 km/h, with an average speed of approximately 21 km/hour. Also, readers should notice that the instantaneous velocity equaling zero takes the highest proportion of the distribution, which indicates that when a train is going through the City of Columbia, it may take several stops, which will complicate the train blockage window predictions, especially for the blockage durations.

The Columbia network OSM map is obtained from OpenStreetMap (https://www.openstreetmap.org/; https://en.wikipedia.org/wiki/OpenStreetMap) and covert it to an XML file. Then the author displays the road network of the City of Columbia, SC in Figure 5.4, with the area in the case study being highlighted. As previously displayed in Table 2.1, there are a total of 7,668 nodes together with 21,502 arcs that will be potentially affected by train blockages. Once the postman starts delivering, the dispatching center must make quick decisions on the order in which customers should be served based on their package delivery priorities and (2) determining the optimal route for the postman, with the objective of minimizing delivery time and avoiding train blockages.

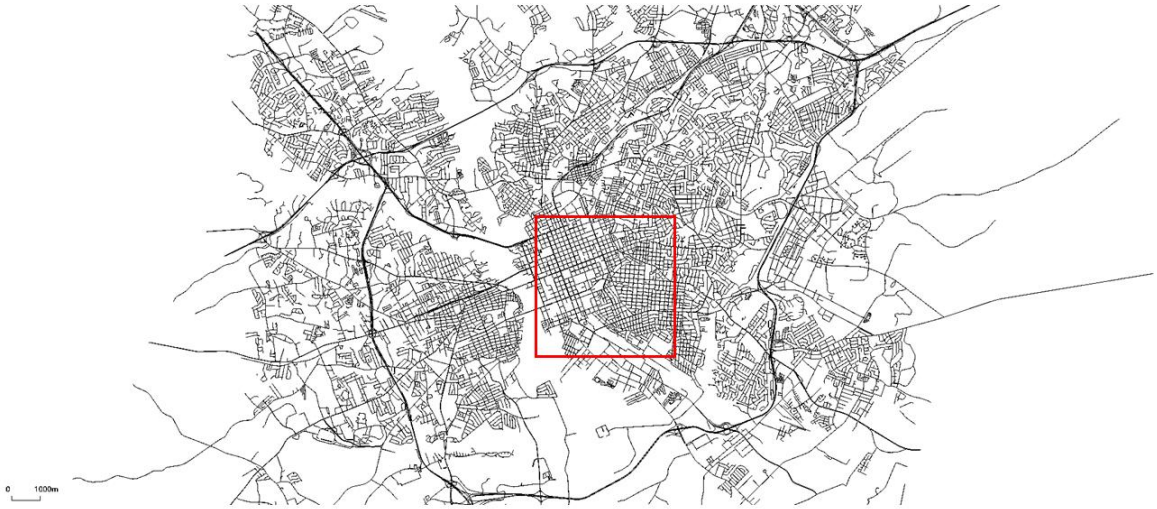

Figure 5.4 Road network of the City of Columbia, SC with highlighted study area (Shown in SUMO).

In addition, the rail network of Columbia is available from the U.S. Census Bureau, Department of Commerce (https://catalog.data.gov/dataset/tiger-line-shapefile-2019-nation-u-s-rails-national-shapefile). To identify grade crossings, the author lays the two networks one over another and compares the crossings. Combining the identified grade crossing information with the real-world freight train operational GPS data shared

by CSX, the author has successfully integrated train blockage information into the last mile delivery routing planning system.

5.2.2 BLOCKAGE WINDOW ESTIMATE

The shortest path problem for last mile deliveries with train blockage windows consists in finding a single-origin and single-destination shortest path in a train crossing network for delivery vehicles, which can be described as follows. Given a directed non-negative weighted graph, $G = (V, A)$, where V is the set of nodes and A is the set of weighted arcs. For each grade crossing node $v \in V$, a blockage window $t_v = [t_v^s, t_v^e]$ will be generated at each node. Variables used in this research are listed in Table 5.2.

Table 5.2 Variables and Definitions.

Set Variables	Description
$G = (V, A)$	Directed non-negative weighted graph
V	The set of nodes in G, $v \in V$
A	The set of weighted arcs/links, $a_{ij} \in A$
Train Related Variables	
l_{train}	Train length
v_{train}^t	Train operating speed at time *t*
$d_{train}^{i,j}$	Train route distance between grade crossing nodes *i* and *j*
$[t_v^s, t_v^e]$	Train blockage window at node *v* starting at $t = t_v^s$ and ending at $t = t_v^e$
Road Network Related Variables	
(r, s)	OD pair, from origin node *r* to destination node *s*
$\bar{t}_{ij}$	The average road traveling time on the arc/link a_{ij}
b_{ij}	A binary variable, $b_{ij} = 1$ if the arc/link a_{ij} is blocked by a train, otherwise, $b_{ij} = 0$
T_v	Accumulative time after an emergency occurs when the emergency vehicle arrives at node *v*
D_v	Expected time delay at node *v*
D_{total}	Total time delay
Decision Variable	
x_{ij}^{rs}	A binary decision variable, $x_{ij}^{rs} = 1$ if the link a_{ij} lies on the path (r, s), otherwise, $x_{ij}^{rs} = 0$

Estimating the train blockage window with precision poses a challenge due to the numerous factors that can result in train operational uncertainties in the real world. These factors encompass variables such as speeding, braking, and even instances of complete stops. Consequently, trains do not always travel at a constant or stable speed, which complicates the precise estimation of the train blockage window.

In this research, the author incorporates the influence of braking time (Zhang et al., 2020) as part of the overall increase in travel time resulting from speed reduction. Therefore, to estimate train blockage windows, some basic train information is needed, such as train length (l_{train}) , current location (d_{train}^{t}), and operating speed (v_{train}^{t}). Given the train information known above, the author assumes that at time $t = t_0$, a train is going through the city. The locomotive is currently at the location $d_{train}^{t_0}$, and the instantaneous speed is $v_{train}^{t_0}$.

It is important to note that trains can change their speed constantly, slow down or even stop completely. As the GPS device records separate instantaneous velocities, we utilize the updated average speed to predict the speed of the train for the next time interval between two recorded instances:

$$\bar{v}_{train}^{t_i} = \frac{d_{train}^{t_i} - d_{train}^{t_0}}{t_i - t_0} \tag{5.1}$$

where i is the time index of the record instances, t_i is the ith recorded time point, $d_{train}^{t_i}$ donates the locomotive location at $t = t_i$.

The GPS data also provides the train locomotive location information, then readers can directly tell how far the train has traveled between two recorded instances:

$$d_i = d_{train}^{t_i} - d_{train}^{t_{i-1}} \tag{5.2}$$

But for any $t \in [t_i, t_{i+1}]$, the estimated traveling distance for the period is needed:

$$d_i^{estimate} = \int_{t_i}^{t_i+\Delta t} v_{train}^t \cdot \Delta t \tag{5.3}$$

According to the principle of integral calculus, the closer Δt to zero, the more accurate the estimation will be. However, in reality, GPS devices cannot record time periods that are extremely close to zero. In implications, the author uses the average speed between two neighboring records instead to estimate $d_{estimate}$.

$$d_i^{estimate} = \bar{v}_{train}^{t_i} \cdot \Delta t \tag{5.4}$$

Then, the estimated start time t_v^{s} of the train blockage window at next grade crossing node v is:

$$t_v^{\mathrm{s}} = t_0 + \frac{D_0 - \sum_i d_i}{\bar{v}_{train}^{t_i}} \tag{5.5}$$

where D_0 stands for the initial distance between the locomotive location and the grade crossing at $t = t_0$.

Then, the duration time of the train blockage can be estimated by:

$$t_{duration} = \frac{l_{train}}{v_{train}^t} \tag{5.6}$$

Therefore, the estimation of the end of the blockage time only need to add the at node v is: (5.6)

$$t_v^{\mathrm{e}} = t_v^{\mathrm{s}} + t_{duration} = t_0 + \frac{l_{train} + D_0 - \sum_i d_i}{\bar{v}_{train}^{t_i}} \tag{5.7}$$

To summarize, to estimate the blockage time of each grade crossing, the basic input data includes the railroad network with identified grade crossings, the current train or locomotive location, the instantaneous train speed, and the length of the train. Here is an

example calculation for a blockage window period estimation when a train is going through a sequence of grade crossings, based on the CSX train GPS data on November 1st, 2020.

(a) T=17:09:10

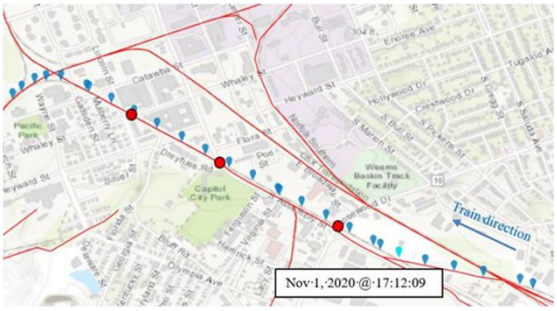

(b) T=17:12:09

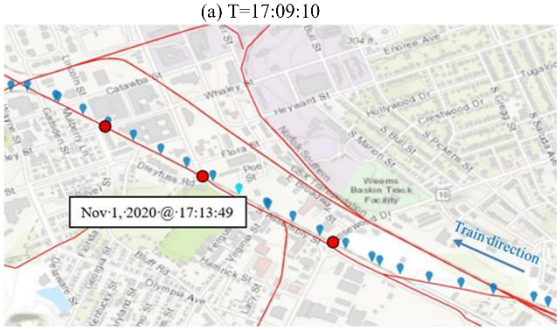

(c) T=17:13:49

Figure 5.5 Blockage Window Estimate Example (Shown in ArcGIS Pro).

Case 1: T=17:09:10

According to the GPS records, in Figure 5.5(a), the locomotive of Train #F772** is located at the position in the figure (light blue highlighted) with an instantaneous velocity of zero at 17:09:10 on November 1, 2020. The train is 5,097 meters long, and it goes through the City of Columbia from the southeast to the west. There are three grade crossings along the train trajectory.

At $t_0 = 17{:}09{:}10$, the locomotive is 1,776 m away from grade crossing #1, and the distances between the first and the second, crossings #2 and #3 are 1,979 m and 1,461 m, respectively.

Therefore, for $t_0 = 17{:}09{:}10$, there will be no estimated blockage windows at three grade crossings, as the train completely stops.

Case 2: T=17:12:09

For $t_1 = 17{:}12{:}09$, as shown in Figure 5.5(b), the instantaneous velocity is 14 m/s, then we can estimate blockage windows at each grade crossings as follows.

For grade crossing #1, the estimated blockage window:

$$t_1^{\mathrm{s}} = t_1 + \frac{D_{0-1} - \sum_i d_i}{\bar{v}_{train}^{t_1}} = 17{:}12{:}09 + \frac{1776 - 752}{\frac{752}{179}} = 17{:}16{:}13$$

$$t_1^{\mathrm{e}} = t_1 + \frac{l_{train} + D_{0-1} - \sum_i d_i}{\bar{v}_{train}^{t_1}} = 17{:}12{:}09 + \frac{5097 + 1776 - 752}{\frac{752}{179}} = 17{:}36{:}25$$

where D_{0-1} donates the initial distance between the train locomotive and the grade crossing #1.

Therefore, the estimated blockage window of grade crossing #1 is [17:16, 17:36].

Similarly, for grade crossing #2:

$$t_2^{\mathrm{s}} = t_1 + \frac{D_{0-2} - \sum_i d_i}{\bar{v}_{train}^{t_1}} = 17{:}12{:}09 + \frac{3755 - 752}{\frac{752}{179}} = 17{:}24{:}07$$

$$t_2^{\mathrm{e}} = t_1 + \frac{l_{train} + D_{0-2} - \sum_i d_i}{\bar{v}_{train}^{t_1}} = 17{:}12{:}09 + \frac{5097 + 3755 - 752}{\frac{752}{179}} = 17{:}44{:}17$$

Hence, the estimated blockage window of grade crossing #2 is [17:24, 17:44].

For grade crossing #3:

$$t_3^{\mathrm{s}} = t_1 + \frac{D_{0-3} - \sum_i d_i}{\bar{v}_{train}^{t_1}} = 17{:}12{:}09 + \frac{5216 - 752}{\frac{752}{179}} = 17{:}29{:}52$$

$$t_3^e = t_1 + \frac{l_{train} + D_{0-3} - \sum_i d_i}{\bar{v}_{train}^{t_1}} = 17{:}12{:}09 + \frac{5097 + 5216 - 752}{\frac{752}{179}} = 17{:}50{:}05$$

The estimated blockage window of grade crossing #3 is [17:30, 17:50].

Case 3: T=17:13:49

For $t_2 = 17{:}13{:}49$, see Figure 5.5(c), the instantaneous velocity is 18 m/s, then the estimated blockage windows are as follows.

In this case, although the train locomotive has passed grade crossing #1, the tail of the train remains behind the crossing, which means the grade crossing is still blocked.

For grade crossing #1:

$$t_1^s = current\ time = 17{:}13{:}49$$

$$t_1^e = t_2 + \frac{l_{train} + D_{0-1} - \sum_i d_i}{\bar{v}_{train}^{t_1}} = 17{:}13{:}49 + \frac{5097 + 1776 - 3171}{\frac{3171}{279}} = 17{:}19{:}15$$

Therefore, the estimated blockage window of grade crossing #1 has been updated from [17:16, 17:36] to [current, 17:19].

For grade crossing #2:

$$t_2^s = t_2 + \frac{D_{0-2} - \sum_i d_i}{\bar{v}_{train}^{t_2}} = 17{:}13{:}49 + \frac{3755 - 3171}{\frac{3171}{279}} = 17{:}14{:}40$$

$$t_2^e = t_2 + \frac{l_{train} + D_{0-2} - \sum_i d_i}{\bar{v}_{train}^{t_2}} = 17{:}13{:}49 + \frac{5097 + 3755 - 3171}{\frac{3171}{279}} = 17{:}22{:}09$$

Hence, the estimated blockage window of grade crossing #2 has been updated from [17:24, 17:44] to [17:15, 17:22].

For grade crossing #3:

$$t_3^{\mathrm{s}} = t_2 + \frac{D_{0-3} - \sum_i d_i}{\bar{v}_{train}^{t_2}} = 17{:}13{:}49 + \frac{5216 - 3171}{\frac{3171}{279}} = 17{:}16{:}49$$

$$t_3^{\mathrm{e}} = t_2 + \frac{l_{train} + D_{0-3} - \sum_i d_i}{\bar{v}_{train}^{t_2}} = 17{:}13{:}49 + \frac{5097 + 5216 - 3171}{\frac{3171}{279}} = 17{:}24{:}17$$

The estimated blockage window of grade crossing #3 has been updated from [17:30, 17:50] to [17:17, 17:24].

This updating process can be consistently applied in cases where new GPS data becomes available, allowing us to adjust the estimated time window for train blockage accordingly.

5.2.3 OPTIMIZATION MODEL

Compared to the traditional shortest path problems, the author will need to modify the model to incorporate train blockage windows. The key step is to update the estimated vehicle arrival time.

$$T_j = \begin{cases} t_v^{\mathrm{e}} \ \ if\ t_v^{\mathrm{s}} < T_i + \bar{t}_{ij} < t_v^{\mathrm{e}} \\ T_i + \bar{t}_{ij}, Otherwise \end{cases}, \forall i, j \in V \tag{5.8}$$

Equation (5.8) estimates the updated arrival time of an emergency vehicle at node j. If the initial arrival time, $T_i + \bar{t}_{ij}$, falls into the train blockage window at the node j, then it will be adjusted to the end of the blockage window.

Then the author can calculate the expected time delay at node v. Generally, the expected delay time at node v can be written as:

$$D_v = \begin{cases} 0, \ \ if\ T_v < t_v^s\ or\ T_v > t_v^e \\ t_v^e - T_v, Otherwise \end{cases} \tag{5.9}$$

Then the total time delay can be calculated as:

$$D_{total} = \sum_{v \in V} D_v \tag{5.10}$$

Initially, the dispatching center is going to find the shortest path with minimum delivery time, then the optimization model can be generated as follows:

$$Z = \min T_s = \min_x \sum_{(i,j)\in A} \left(T_j - T_i\right) \cdot x_{ij}^{rs}, \forall r, s \in V \tag{5.11}$$

s.t.

$$\sum_j x_{ij}^{rs} - \sum_i x_{ij}^{rs} = \begin{cases} 1, & \forall i = r \\ 0, & \forall i \neq r, \forall j = s \\ -1, & \forall j = s \end{cases} \tag{5.12}$$

$$x_{ij}^{rs} = \begin{cases} 1, if\ a_{ij} \text{ lies on the path } (r,s) \\ 0, otherwise \end{cases}, \forall a_{ij} \in A, \forall r, s \in V \tag{5.13}$$

The objective function (5.11) minimizes the cumulative delivery time when the postman finally arrives at the last customer node after he departs from the local store. Equation (5.12) represents the flow balance constraints for a path between the origin node r and the destination node s. For example, any intermediate nodes except the origin (the local store) and destination (the last customer node) should satisfy flow-in equals to flow-out. For the origin node, flow-out equals to one without flow-in. Similarly for the destination node, flow-in equals to one without flow-out. Equation (5.13) defines the binary decision variable.

Considering that mathematically minimizing the total response time equals minimizing the total delay time in Equation (5.10), then the original optimization model can be rewritten as:

$$\min D_{total} = \min_x \sum_{(i,j)\in A} D_j \cdot x_{ij}^{rs}, \forall r, s \in V \tag{5.14}$$

s.t.

$$\sum_j x_{ij}^{rs} - \sum_i x_{ij}^{rs} = \begin{cases} 1, & \forall i = r \\ 0, & \forall i \neq r, \forall j = s \\ -1, & \forall j = s \end{cases} \quad (5.15)$$

$$x_{ij}^{rs} = \begin{cases} 1, if\ a_{ij} \text{ lies on the path } (r,s) \\ 0, otherwise \end{cases}, \forall a_{ij} \in A, \forall r, s \in V \quad (5.16)$$

The objective function (5.14) calculates and then minimizes the total time delay when the emergency vehicle goes through each node on the path. Equation (5.15) represents the flow balance constraints for a path between the origin node r and the destination node s. Equation (5.16) defines the binary decision variable.

5.2.4 MODIFIED LABEL CORRECTING ALGORITHM

The performance of the shortest path algorithms is heavily dependent on the sparseness of the network, list processing and network representation, and distance measures on the arcs (Golden, 1976). Some classical shortest path algorithms like Dijkstra and Floyd algorithms have a high time complexity, and Dijkstra algorithm is also limited to non-negative weight problems (Golden, 1976; Zhao and Zhao, 2017). Compared to these algorithms, the label correcting algorithm is more time efficient (Bertsekas, 1993; Kergosien et al., 2022; Sedeño-Noda and González-Martín, 2012), especially for dynamic approximate shortest path problems (Karczmarz and Łącki, 2019; Lawson et al., 2013). In the context of this research, any logistical store can be treated as a distinct origin node, all other nodes represent potential customer nodes where the package should be delivered, while the travel time on some edges/arcs can be dynamically changed due to the potential train blockages. Thus, the label correcting algorithm is well-suited for the generation of shortest paths in these scenarios.

In classical single source shortest paths algorithms, the process typically begins by initializing the distance matrix with $d(s) = 0, d(v) = \infty$ for any other node $v \in$

$V\backslash\{s\}$, where s is the source node. The algorithm then proceeds with edge relaxations, which involve updating the distances by setting $d(v) = d(u) + c(u,v)$ if $d(v) < d(u) + c(u,v)$ where $u \in V, d(u) \neq \infty$, and $c(u,v)$ represents the cost of the edge or arc connecting nodes u and v. These relaxations are performed on tense edges until no more tense edges exist, resulting in the distance matrix $\boldsymbol{d}$ representing the distances from the source node (Karczmarz and Łącki, 2019).

In traditional shortest path algorithms, the edge cost $c(u,v)$ is typically a constant value. However, in this research, the edge cost $c(u,v)$ can be changed due to the potential delay caused by the train blockages, as indicated in Equations (5.8) and (5.9), when node u corresponds to a grade crossing. Consequently, the author identifies all the grade crossings first, and then detects if the estimated vehicle arrival time at grade crossings should fall into the blockage window. If the estimated vehicle arrival time at a grade crossing falls within the blockage window, it indicates that the delivery vehicle will be blocked by a passing train. In such cases, the framework proceeds to update the actual departure time from the grade crossing using the end of the train blockage window, instead of the original estimated arrival time. This consideration allows for the incorporation of the potential blockage delays into the shortest path calculations, enhancing the algorithm's ability to find the optimal routes considering train blockages.

The flowchart for the modified label correcting algorithm is provided in Figure 5.6.

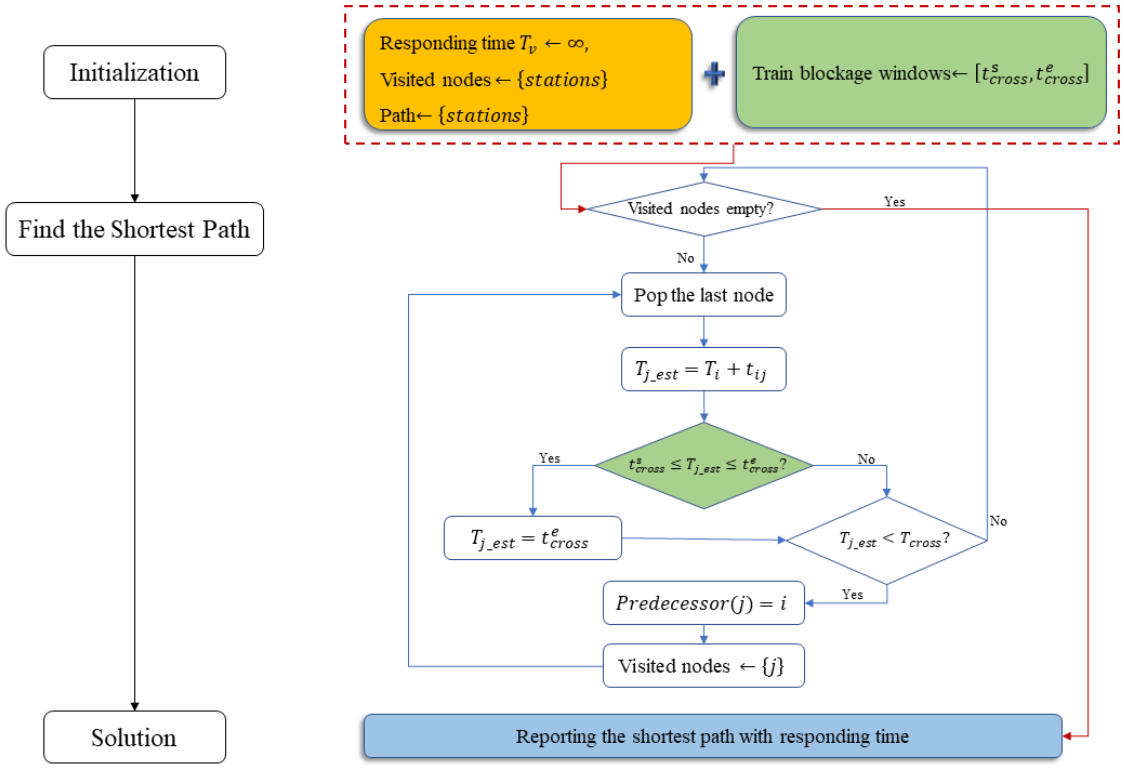

Figure 5.6 Flowchart of the modified label correcting algorithm.

5.3 CASE STUDY AND RESULTS

A case study of the last mile delivery problem with train blockage from the City of Columbia, SC is presented in this section. Assume there are two separate trains going through the city, with estimated blockage windows in Table 5.3 and there will be a five-min processing time for the postman at each customer node. The geographical locations of a United States Postal Service (USPS) store and three customers are displayed in Figure 5.7. If the train blockage is not considered, the shortest delivery path is shown in Figure 5.8, which serves as the baseline path, with a more detailed path summary in Table 5.4.

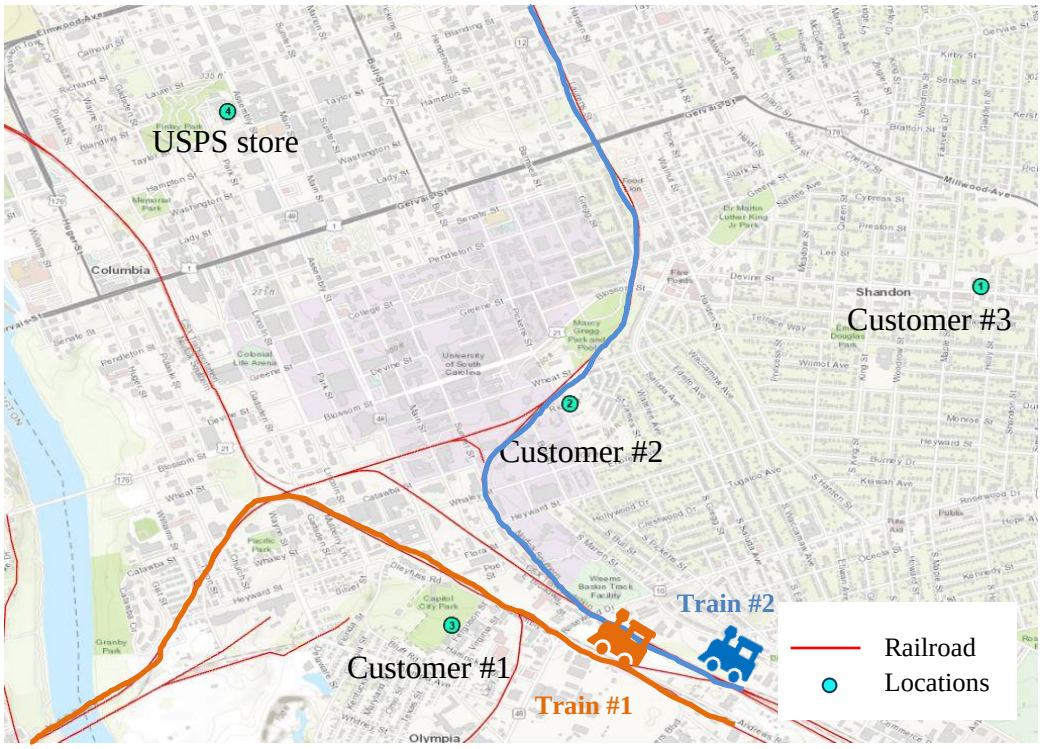

Figure 5.7 Locations of USPS store and Customers (Shown in ArcGIS Pro).

Table 5.3 Train blockage windows at grade crossings.

Train #1 Departing at 9 am		Train #2 Departing at 9:09 am	
Nodes	Blockage Windows	Nodes	Blockage Windows
2750	[9:00, 9:14]	7062	[9:09, 9:29]
1331	[9:01, 9:15]	3995	[9:12, 9:30]
1332	[9:01, 9:19]	1303	[9:13, 9:31]
4041	[9:04, 9:41]	1728	[9:15, 9:32]
7297	[9:07, 9:42]	6348	[9:16, 9:34]
1734	[9:08, 9:45]	1730	[9:19, 9:36]
4006	[9:48, 10:04]	6523	[9:20, 9:51]
2944	[9:52, 10:08]	1414	[9:36, 10:01]
3887	[9:55, 10:09]	3234	[9:44, 10:02]

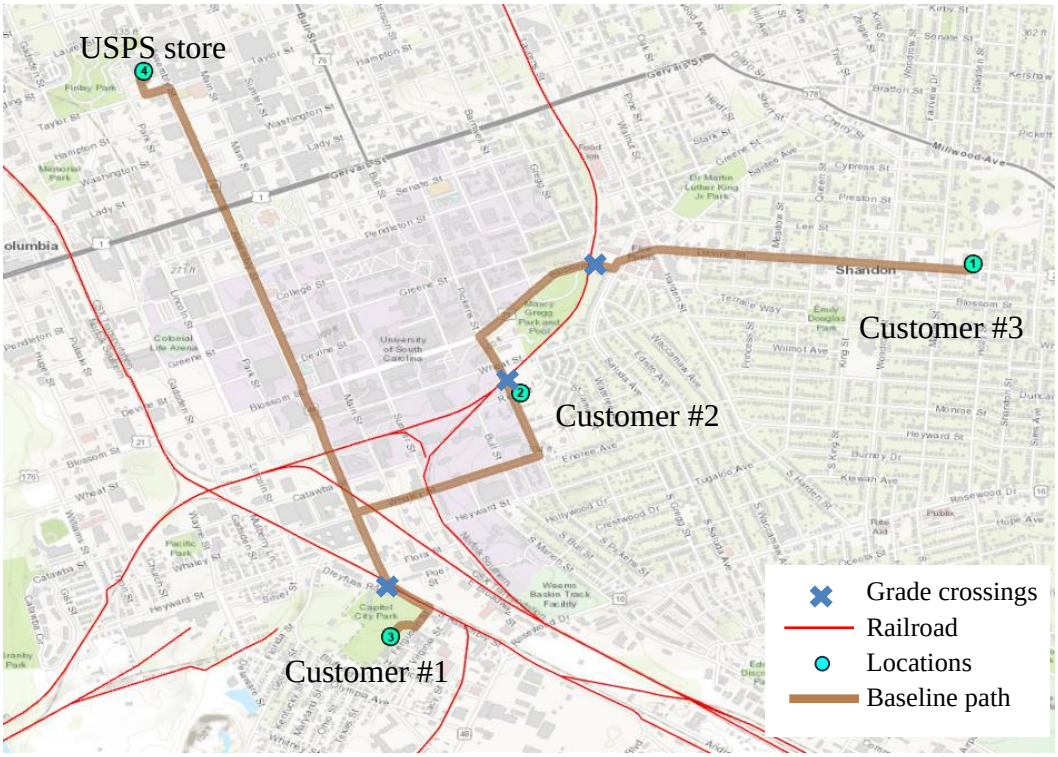

Figure 5.8 The shortest delivery path without train blockages (Shown in ArcGIS Pro).

Table 5.4 Summary on the baseline path.

Deliveries	Path	Distance/km	Time/min
USPS to Customer #1	7635, 7465, 7500, 7363, 7345, 7560, 7312, 7571, 7634, 3960, 7658, 5355, 3650, 3958, 6417, **4041**[1], 4042, 4043, 4894, 4893	3.09	3.84 (+5)[2]
Customer #1 to #2	4893, 4894, 4043, 4042, **4041**[1], 6417, 3958, 7525, 7332, 3146, 4450, 3993, 3652, 3994	1.91	2.20 (+5)[2]
Customer #2 to #3	3994, **3995**[1], 3996, 7633, 6701, 1295, 2868, 6818, **1728**[1], 5416, 6336, 7556, 5375, 6816, 5377, 1313, 4549, 4000, 4929, 4656, 3382, 3361, 2528	2.60	3.26 (+5)[2]
	Sum	7.60	9.30 (+15)[2]

Note: 1. The nodes that are both bolded and underlined represent the grade crossings.
2: A five-min processing time at each customer node.

Figure 5.8 clearly shows that when the postman follows the baseline path, there is a potential for him to be blocked on his way to the customers. Alternatively, if the train blockages are taken into consideration, the proposed modified label correcting algorithm can determine the time-based shortest path based on the departure time from the USPS store.

5.3.1 SCENARIO #1: DEPART AT 9:00 AM

In this scenario, the author assumes the postman begins package delivery to customers from the USPS store at 9:00 a.m. If the postman follows the baseline path shown in Figure 5.8 and considering the travel time information provided in Table 5.4, it becomes evident that the postman will encounter a blockage at Node #4041 (arriving at the node at 9:10 a.m., while the train blockage window is [9:04, 9:41]) due to a passing train during his second delivery, while traveling from Customer #1 to Customer #2. And similarly for the third delivery, the postman will encounter blockages at both Node #3995 (arriving at the node at 9:16 a.m., within the train blockage window of [9:12, 9:30]) and Node #1728 (arriving at the node at 9:18 a.m., within the train blockage window of [9:15, 9:32]).

To avoid potential train blockages and guarantee just-in-time delivery, the proposed algorithm will find a new path for the postman, with minimum travel time as presented in Figure 5.9, with a more detailed path summary in Table 5.5.

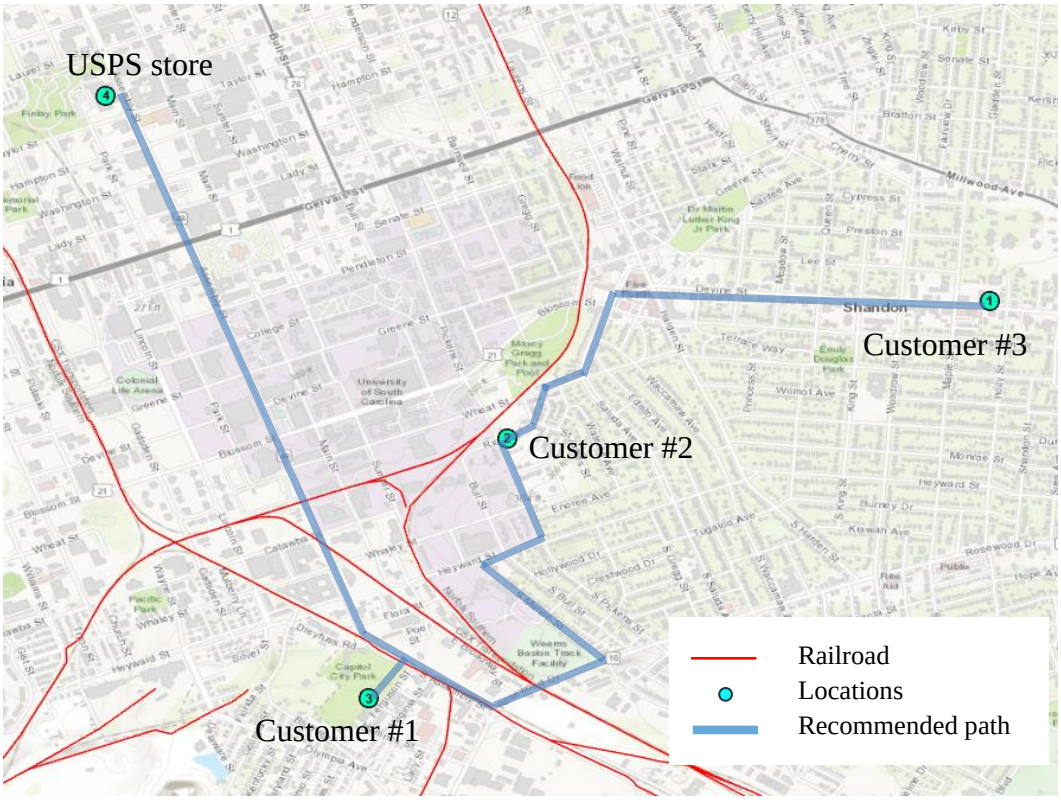

Figure 5.9 Recommended path at 9:00 a.m. (Shown in ArcGIS Pro).

Table 5.5 Summary on the recommended path at 9:00 a.m.

Deliveries	Path	Distance/km	Time/min
USPS to Customer #1	7635, 7465, 7500, 7363, 7345, 7560, 7312, 7571, 7634, 3960, 7658, 5355, 3650, 3958, 6417, **4041**[1], 4042, 4043, 4894, 4893	3.09	3.84 (+5)[2]
Customer #1 to #2	4893, 4894, 4043, 4044, 1101, 7013, 7012, 7011, 7010, 7008, 7007, 7469, 3008, 4655, 1840, 1841, 1842, 2406, 7418, 3992, 3993, 3652, 3994	2.45	3.95 (+5)[2]
Customer #2 to #3	3994, 1302, 2556, 2555, 2865, 7528, 6335, 2995, 6336, 7556, 5375, 6816, 5377, 1313, 4549, 4000, 4929, 4656, 3382, 3361, 2528	2.48	3.44 (+5)[2]
	Sum	8.02	11.23 (+15)[2]

Note: 1. The nodes that are both bolded and underlined represent the grade crossings.
2: A five-min processing time at each customer node.

5.3.2 SCENARIO #2: DEPART AT 9:15 AM

In this scenario, the author assumes the postman begins package delivery to customers from the USPS store at 9:15 a.m. If the postman follows the baseline path shown in Figure 5.8 and considering the travel time information provided in Table 5.4, it is clear to assert that the postman will be blocked at Node #4041 (arriving at the node at 9:18 while the train blockage window is [9:04, 9:41]) by the train during his first delivery traveling from the USPS store to Customer #1.

Similarly, the algorithm will try to recommend another path for the postman with minimum travel time under the current circumstance, see Figure 5.10, with a more detailed path summary in Table 5.6.

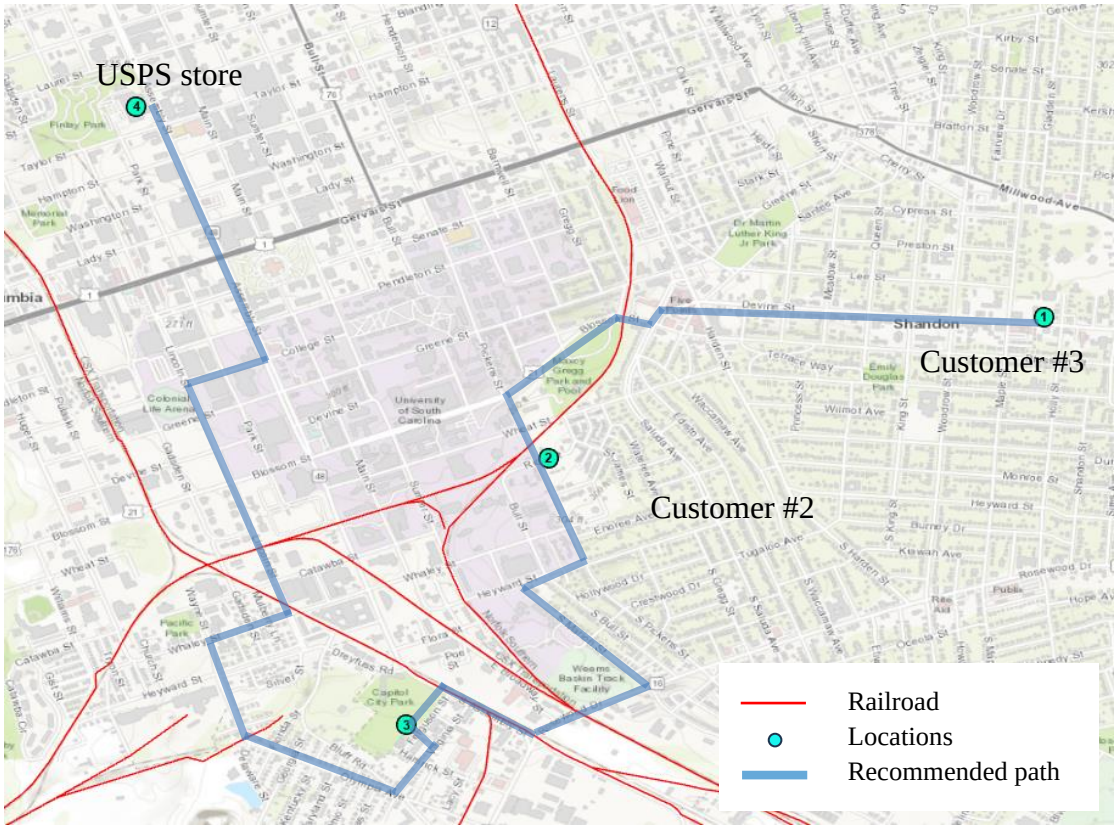

Figure 5.10 Recommended path at 9:15 a.m. (Shown in ArcGIS Pro).

Table 5.6 Summary on the recommended path at 9:15 a.m.

Deliveries	Path	Distance/km	Time/min
USPS to Customer #1	7635, 7465, 7500, 7363, 7345, 7560, 7312, 7571, 1254, 7630, 7506, 7629, 7631, 5925, 945, **7297**[1], 1733, 3018, 4512, 7431, 5287, 7509, 7511, 7340, 7459, 7420, 7554, 7434, 7521, 4703, 6956, 4704, 4705, 4893	4.43	5.19 (+5)[2]
Customer #1 to #2	4893, 4894, 4043, 4044, 1101, 7013, 7012, 7011, 7010, 7008, 7007, 7469, 3008, 4655, 1840, 1841, 1842, 2406, 7418, 3992, 3993, 3652, 3994	2.45	3.95 (+5)[2]
Customer #2 to #3	3994, **3995**[1], 3996, 7633, 6701, 1295, 2868, 6818, **1728**[1], 5416, 6336, 7556, 5375, 6816, 5377, 1313, 4549, 4000, 4929, 4656, 3382, 3361, 2528	2.60	3.26 (+5)[2]
	Sum	9.48	12.40 (+15)[2]

Note: 1. The nodes that are both bolded and underlined represent the grade crossings.
2: A five-min processing time at each customer node.

5.3.3 SCENARIO #3: DEPART AT 9:30 AM

In this scenario, the author assumes the postman begins package delivery to customers from the USPS store at 9:30 a.m. If the postman follows the baseline path shown in Figure 5.8 and considering the travel time information provided in Table 5.4, it is clear to assert that the postman will be blocked at Node #4041 (arriving at the node at 9:33 while the train blockage window is [9:04, 9:41]) by the train during his first delivery traveling from the USPS store to Customer #1.

Similarly, the algorithm will try to recommend another path for the postman with minimum travel time under the current circumstance, see Figure 5.11, with a more detailed path summary in Table 5.7.

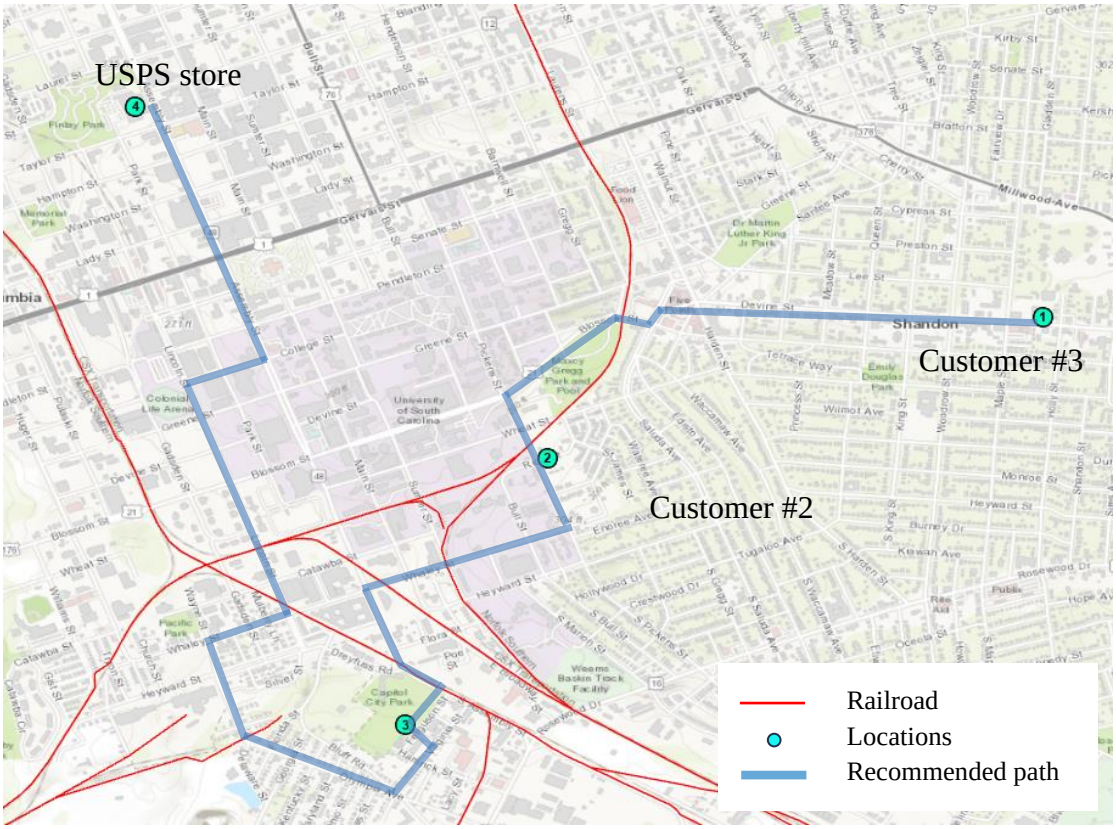

Figure 5.11 Recommended path at 9:30 a.m. (Shown in ArcGIS Pro).

Table 5.7 Summary on the recommended path at 9:30 a.m.

Deliveries	Path	Distance/km	Time/min
USPS to Customer #1	7635, 7465, 7500, 7363, 7345, 7560, 7312, 7571, 1254, 7630, 7506, 7629, 7631, 5925, 945, **7297**[1], 1733, 3018, 4512, 7431, 5287, 7509, 7511, 7340, 7459, 7420, 7554, 7434, 7521, 4703, 6956, 4704, 4705, 4893	4.43	5.19 (+5)[2]
Customer #1 to #2	4893, 4894, 4043, 4042, 40411, 6417, 3958, 7525, 7332, 3146, 4450, 3993, 3652, 3994	1.91	2.20 (+5)2
Customer #2 to #3	3994, 39951, 3996, 7633, 6701, 1295, 2868, 6818, 17281, 5416, 6336, 7556, 5375, 6816, 5377, 1313, 4549, 4000, 4929, 4656, 3382, 3361, 2528	2.60	3.26 (+5)2
	Sum	8.94	10.65 (+15)[2]

Note: 1. The nodes that are both bolded and underlined represent the grade crossings.
2: A five-min processing time at each customer node.

5.3.4 SCENARIO #4: DEPART AT 9:45 AM

In this scenario, the author assumes the postman begins package delivery to customers from the USPS store at 9:45 a.m., a time when both trains have already passed through the city. Consequently, in this scenario, the postman can deliver to all the customers by following the baseline path without encountering any train blockages and the algorithm recommended path is completely as the baseline path shown in Figure 5.8 and path information descried in Table 5.4.

5.3.5 RESULTS COMPARISONS

To make comparisons of the three scenarios above, a baseline time is calculated based on the principle that the postman follows the baseline path and will wait until the traffic is clear when there is a train blockage. The author reports the time delay in Table 5.5.

Table 5.8 Time saved from the baseline.

	Scenario #1	Scenario #2	Scenario #3	Scenario #4
Baseline path/min	45.74	48.19	33.19	24.30
Recommended path/min	26.23	27.40	25.65	24.30
Time saved/min	19.51	20.79	7.54	0.00
Time saved percentage	42.6%	43.1%	22.7%	0%

Note: Time calculations in this table include a total of 15 minutes for the postman's processing at three customers.

5.4 CONCLUSIONS

This research investigates shortest path problems for last mile deliveries with train blockages by filling the knowledge gap that limited literature has focused on the impact of train blockage on road networks. The author proposes an optimization model and develops the corresponding algorithm based on the Label Correcting method. A case study at the City of Columbia, South Carolina, has been conducted to verify the

effectiveness and robustness of the model. The results indicate a saving up to 43.1% of the time by considering train blockages compared to the current practice, in which the crossing blockage information is unavailable.

In the results section, the author presents various scenarios that demonstrate the effectiveness of the model in dispatching first responder vehicles from the fire department stations under different train blockage conditions. This indicates that the algorithm is robust and capable of addressing real-world situations. Furthermore, since the model utilizes the framework depicted in Figure 5.1, its implementation can be easily adapted and extended to other cities or road-rail networks. This adaptability is feasible as long as the necessary foundational data and information, including road and railroad networks, as well as train operational data, are accessible. In conclusion, this framework provides a valuable tool for optimizing the dispatch of first responder vehicles in the presence of train blockages. The obtained results from the scenarios indicate that the time-dependent shortest path and the distance-based shortest path can sometimes differ for the same destination. This discrepancy arises when the distance-based shortest paths from alternative origins are blocked, causing the second or even the third shortest path to become the most time-efficient route temporarily. The findings emphasize the importance of considering potential train blockages in optimizing the dispatch of emergency vehicles. By doing so, the author can identify the most time-efficient routes and significantly improve last mile delivery just-in-time efforts.

This study also demonstrates the importance and benefit of the different agencies and private sectors sharing vital information for the connected community and improved mobility. Meanwhile, this research paves the path for the future integration of railroad

information into the grand intelligent transportation system, especially when the positive train control system is fully implemented.

Despite the contributions of this research, there are still some limitations that should be mentioned. Firstly, although a mathematical model is proposed to estimate train blockage windows, it is still more than arduous to precisely have the train blockage windows. But this could be solved in the future once a secured and reliable communication channel can be established between the railroads and the dispatching centers. Secondly, this research has not considered any delay due to traffic congestion or traffic lights. Some other stochastic factors, such as weather conditions, left turns versus right turns, and height limits, will also inevitably affect the delivery time, which have not been taken into consideration in this research.

REFERENCES

36 Automotive Industry Statistics [2023]: Average Employment, Sales, And More, 2023. . Zippia. URL https://www.zippia.com/advice/automotive-industry-statistics/ (accessed 10.9.23).

Advanced Clean Fleets Regulation - Drayage Truck Requirements | California Air Resources Board [WWW Document], 2023. URL https://ww2.arb.ca.gov/resources/fact-sheets/advanced-clean-fleets-regulation-drayage-truck-requirements (accessed 10.10.23).

Amiri, A., Amin, S.H., Zolfagharinia, H., 2023. A bi-objective green vehicle routing problem with a mixed fleet of conventional and electric trucks: Considering charging power and density of stations. Expert Systems with Applications 213, 119228. https://doi.org/10.1016/j.eswa.2022.119228

Awerbuch, B., Bar-Noy, A., Gopal, M., 1994. Approximate distributed Bellman-Ford algorithms. IEEE Transactions on Communications 42, 2515–2517. https://doi.org/10.1109/26.310604

Baertlein, L., Baertlein, L., 2023. Focus: California's port truck-charging plan gets a jolt from big investors. Reuters.

Beard-Raymond, M., Farzaneh, M., Duran, C., Zietsman, J., Lee, D.-W., Johnson, J., 2009. SmartWay Applications for Drayage Trucks 50.

Bellman, R.E., Dreyfus, S.E., 2015. Applied Dynamic Programming, Applied Dynamic Programming. Princeton University Press.

Bertsekas, D.P., 1993. A simple and fast label correcting algorithm for shortest paths. Networks 23, 703–709. https://doi.org/10.1002/net.3230230808

Braekers, K., Ramaekers, K., Van Nieuwenhuyse, I., 2016. The vehicle routing problem: State of the art classification and review. Computers & Industrial Engineering 99, 300–313. https://doi.org/10.1016/j.cie.2015.12.007

Bräysy, O., Dullaert, W., Gendreau, M., 2004. Evolutionary Algorithms for the Vehicle Routing Problem with Time Windows. J Heuristics 10, 587–611. https://doi.org/10.1007/s10732-005-5431-6

Budde-Meiwes, H., Drillkens, J., Lunz, B., Muennix, J., Rothgang, S., Kowal, J., Sauer, D.U., 2013. A review of current automotive battery technology and future

prospects. Proceedings of the Institution of Mechanical Engineers, Part D: Journal of Automobile Engineering 227, 761–776. https://doi.org/10.1177/0954407013485567

Çabukoglu, E., Georges, G., Küng, L., Pareschi, G., Boulouchos, K., 2018. Battery electric propulsion: An option for heavy-duty vehicles? Results from a Swiss case-study. Transportation Research Part C: Emerging Technologies 88, 107–123. https://doi.org/10.1016/j.trc.2018.01.013

Carrabs, F., D'Ambrosio, C., Ferone, D., Festa, P., Laureana, F., 2020. The constrained forward shortest path tour problem: Mathematical modeling and GRASP approximate solutions. Networks 78, 17–31. https://doi.org/10.1002/net.22010

Chassein, A., Dokka, T., Goerigk, M., 2019. Algorithms and uncertainty sets for data-driven robust shortest path problems. European Journal of Operational Research 274, 671–686. https://doi.org/10.1016/j.ejor.2018.10.006

Chen, G., Govindan, K., Yang, Z., 2013. Managing truck arrivals with time windows to alleviate gate congestion at container terminals. International Journal of Production Economics, Meta-heuristics for manufacturing scheduling and logistics problems 141, 179–188. https://doi.org/10.1016/j.ijpe.2012.03.033

Chen, Y., Wu, X., Hu, K., Borken-Kleefeld, J., 2023. Nox emissions from diesel cars increase with altitude. Transportation Research Part D: Transport and Environment 115, 103573. https://doi.org/10.1016/j.trd.2022.103573

Chen, Y., Zhang, Y., Fan, Y., Hu, K., Zhao, J., 2017. A dynamic programming approach for modeling low-carbon fuel technology adoption considering learning-by-doing effect. Applied Energy 185, 825–835. https://doi.org/10.1016/j.apenergy.2016.10.094

Chiang, W.-C., Russell, R.A., 1996. Simulated annealing metaheuristics for the vehicle routing problem with time windows. Ann Oper Res 63, 3–27. https://doi.org/10.1007/BF02601637

Choi, E., Tcha, D.-W., 2007. A column generation approach to the heterogeneous fleet vehicle routing problem. Computers & Operations Research 34, 2080–2095. https://doi.org/10.1016/j.cor.2005.08.002

Conrad, R.G., Figliozzi, M.A., 2011. The Recharging Vehicle Routing Problem. Presented at the Proceedings of the 2011 industrial engineering research conference, IISE, Norcross, GA.

Desaulniers, G., Madsen, O.B.G., Ropke, S., 2014. Chapter 5: The Vehicle Routing Problem with Time Windows, in: Vehicle Routing, MOS-SIAM Series on Optimization. Society for Industrial and Applied Mathematics, pp. 119–159. https://doi.org/10.1137/1.9781611973594.ch5

Dessouky, M., Yao, S., 2023. Routing of Battery Electric Heavy Duty-Trucks for Drayage Operations. https://doi.org/10.7922/G27M068R

Di Puglia Pugliese, L., Ferone, D., Festa, P., Guerriero, F., 2020. Shortest path tour problem with time windows. European Journal of Operational Research 282, 334–344. https://doi.org/10.1016/j.ejor.2019.08.052

Dijkstra, E.W., 1959. A note on two problems in connexion with graphs. Numerische Mathematik 269–271.

Dreyfus, S.E., 1969. An Appraisal of Some Shortest-Path Algorithms. Operations Research 17, 395–412. https://doi.org/10.1287/opre.17.3.395

Earl, T., Mathieu, L., Cornelis, S., Kenny, S., Ambel, C.C., Nix, J., 2018. Analysis of long haul battery electric trucks in EU 22.

El-Sherbeny, N.A., 2014. The Algorithm of the Time-Dependent Shortest Path Problem with Time Windows. Applied Mathematics 05, 2764. https://doi.org/10.4236/am.2014.517264

Eyring, V., Köhler, H.W., Aardenne, J. van, Lauer, A., 2005. Emissions from international shipping: 1. The last 50 years. Journal of Geophysical Research: Atmospheres 110. https://doi.org/10.1029/2004JD005619

Felipe, Á., Ortuño, M.T., Righini, G., Tirado, G., 2014. A heuristic approach for the green vehicle routing problem with multiple technologies and partial recharges. Transportation Research Part E: Logistics and Transportation Review 71, 111–128. https://doi.org/10.1016/j.tre.2014.09.003

Ferone, D., Festa, P., Guerriero, F., 2020. An efficient exact approach for the constrained shortest path tour problem. Optimization Methods and Software 35, 1–20. https://doi.org/10.1080/10556788.2018.1548015

Filippo, J.D., Callahan, C., Golestani, N., 2019. Zero-Emission Drayage Trucks 60.

FRA, U.Depart. of T., 2022. Highway-Rail Grade Crossing and Trespassing Research | FRA [WWW Document]. URL https://railroads.dot.gov/research-development/program-areas/highway-rail-grade-crossing/highway-rail-grade-crossing-and (accessed 5.30.23).

FRA, U.Depart. of T., 2006. Impact of Blocked Highway/Rail Grade Crossings On Emergency Response Services.

Golden, B., 1976. Technical Note—Shortest-Path Algorithms: A Comparison. Operations Research 24, 1164–1168. https://doi.org/10.1287/opre.24.6.1164

Hiermann, G., Puchinger, J., Ropke, S., Hartl, R.F., 2016. The Electric Fleet Size and Mix Vehicle Routing Problem with Time Windows and Recharging Stations. European Journal of Operational Research 252, 995–1018. https://doi.org/10.1016/j.ejor.2016.01.038

Hilleary, T.N., ByStep, L., 2012. A radar vehicle detection system for four-quadrant gate warning systems and blocked crossing detection. (No. DOT/FRA/ORD-12/24).

Hurtado-Beltran, A., Rilett, L.R., Nam, Y., 2021. Driving Coverage of Charging Stations for Battery Electric Trucks Located at Truck Stop Facilities. Transportation Research Record 2675, 850–866. https://doi.org/10.1177/03611981211031542

Husing, J.E., Brightbill, T.E., Crosby, P.A., 2007. San Pedro Bay Ports Clean Air Action Plan. Economic Analysis: Proposed Clean Trucks Program 108.

Huynh, N., Smith, D., Harder, F., 2016. Truck Appointment Systems: Where We Are and Where to Go from Here. Transportation Research Record 2548, 1–9. https://doi.org/10.3141/2548-01

Jiang, M., Zhang, Y., Zhang, Y., Zhang, C., Zhang, K., Zhang, G., Zhao, Z., 2018. Operation and Scheduling of Pure Electric Buses under Regular Charging Mode, in: 2018 21st International Conference on Intelligent Transportation Systems (ITSC). Presented at the 2018 21st International Conference on Intelligent Transportation Systems (ITSC), pp. 1894–1899. https://doi.org/10.1109/ITSC.2018.8569667

Johnson, D.B., 1973. A Note on Dijkstra's Shortest Path Algorithm. J. ACM 20, 385–388. https://doi.org/10.1145/321765.321768

Juhász, J., Bányai, T., 2018. Last mile logistics: an integrated view. IOP Conf. Ser.: Mater. Sci. Eng. 448, 012026. https://doi.org/10.1088/1757-899X/448/1/012026

Karczmarz, A., Łącki, J., 2019. Simple Label-Correcting Algorithms for Partially Dynamic Approximate Shortest Paths in Directed Graphs, in: Symposium on Simplicity in Algorithms (SOSA), Proceedings. Society for Industrial and Applied Mathematics, pp. 106–120. https://doi.org/10.1137/1.9781611976014.15

Ke, B.-R., Chung, C.-Y., Chen, Y.-C., 2016. Minimizing the costs of constructing an all plug-in electric bus transportation system: A case study in Penghu. Applied Energy 177, 649–660. https://doi.org/10.1016/j.apenergy.2016.05.152

Kergosien, Y., Giret, A., Néron, E., Sauvanet, G., 2022. An Efficient Label-Correcting Algorithm for the Multiobjective Shortest Path Problem. INFORMS Journal on Computing 34, 76–92. https://doi.org/10.1287/ijoc.2021.1081

Kim, J., Rahimi, M., Newell, J., 2012. Life-Cycle Emissions from Port Electrification: A Case Study of Cargo Handling Tractors at the Port of Los Angeles. International

Journal of Sustainable Transportation 6, 321–337. https://doi.org/10.1080/15568318.2011.606353

Kim, Y.J., Chung, B.D., 2023. Energy consumption optimization for the electric vehicle routing problem with state-of-charge-dependent discharging rates. Journal of Cleaner Production 385, 135703. https://doi.org/10.1016/j.jclepro.2022.135703

Laporte, G., 1992. The vehicle routing problem: An overview of exact and approximate algorithms. European Journal of Operational Research 59, 345–358. https://doi.org/10.1016/0377-2217(92)90192-C

Lawson, G., Allen, S., Rose, G., Nguyen, D., Ng, M., 2013. Parallel Label-Correcting Algorithms for Large-Scale Static and Dynamic Transportation Networks on Laptop Personal Computers. Presented at the Transportation Research Board 92nd Annual MeetingTransportation Research Board.

Lee, C., 2021. An exact algorithm for the electric-vehicle routing problem with nonlinear charging time. Journal of the Operational Research Society 72, 1461–1485. https://doi.org/10.1080/01605682.2020.1730250

Lenstra, J.K., Kan, A.H.G.R., 1981. Complexity of vehicle routing and scheduling problems. Networks 11, 221–227. https://doi.org/10.1002/net.3230110211

Li, J.-Q., 2014. Transit Bus Scheduling with Limited Energy. Transportation Science 48, 521–539. https://doi.org/10.1287/trsc.2013.0468

Liimatainen, H., van Vliet, O., Aplyn, D., 2019. The potential of electric trucks – An international commodity-level analysis. Applied Energy 236, 804–814. https://doi.org/10.1016/j.apenergy.2018.12.017

Lopes, R.B., Ferreira, C., Santos, B.S., Barreto, S., 2013. A taxonomical analysis, current methods and objectives on location-routing problems. International Transactions in Operational Research 20, 795–822. https://doi.org/10.1111/itor.12032

Lu, C.-C., Yan, S., Huang, Y.-W., 2018. Optimal scheduling of a taxi fleet with mixed electric and gasoline vehicles to service advance reservations. Transportation Research Part C: Emerging Technologies 93, 479–500. https://doi.org/10.1016/j.trc.2018.06.015

Ma, J., Li, Y., Grundish, N.S., Goodenough, J.B., Chen, Y., Guo, L., Peng, Z., Qi, X., Yang, F., Qie, L., Wang, C.-A., Huang, B., Huang, Z., Chen, L., Su, D., Wang, G., Peng, X., Chen, Z., Yang, J., He, S., Zhang, X., Yu, H., Fu, C., Jiang, M., Deng, W., Sun, C.-F., Pan, Q., Tang, Y., Li, X., Ji, X., Wan, F., Niu, Z., Lian, F., Wang, C., Wallace, G.G., Fan, M., Meng, Q., Xin, S., Guo, Y.-G., Wan, L.-J., 2021. The 2021 battery technology roadmap. J. Phys. D: Appl. Phys. 54, 183001. https://doi.org/10.1088/1361-6463/abd353

Macrina, G., Laporte, G., Guerriero, F., Di Puglia Pugliese, L., 2019. An energy-efficient green-vehicle routing problem with mixed vehicle fleet, partial battery recharging and time windows. European Journal of Operational Research 276, 971–982. https://doi.org/10.1016/j.ejor.2019.01.067

Manthiram, A., 2017. An Outlook on Lithium Ion Battery Technology. ACS Cent. Sci. 3, 1063–1069. https://doi.org/10.1021/acscentsci.7b00288

Manzetti, S., Mariasiu, F., 2015. Electric vehicle battery technologies: From present state to future systems. Renewable and Sustainable Energy Reviews 51, 1004–1012. https://doi.org/10.1016/j.rser.2015.07.010

Mara, S.T.W., Kuo, R. j., Asih, A.M.S., 2021. Location-routing problem: a classification of recent research. International Transactions in Operational Research 28, 2941–2983. https://doi.org/10.1111/itor.12950

Mohamed, A.A.S., Jun, M., Mahmud, R., Mishra, P., Patel, S.N., Tolbert, I., Santhanagopalan, S., Meintz, A., 2022. Hierarchical Control of Megawatt-Scale Charging Stations for Electric Trucks with Distributed Energy Resources. IEEE Transactions on Transportation Electrification 1–1. https://doi.org/10.1109/TTE.2022.3167647

Montoya, A., Guéret, C., Mendoza, J.E., Villegas, J.G., 2017a. The electric vehicle routing problem with nonlinear charging function. Transportation Research Part B: Methodological, Green Urban Transportation 103, 87–110. https://doi.org/10.1016/j.trb.2017.02.004

Montoya, A., Guéret, C., Mendoza, J.E., Villegas, J.G., 2017b. The electric vehicle routing problem with nonlinear charging function. Transportation Research Part B: Methodological, Green Urban Transportation 103, 87–110. https://doi.org/10.1016/j.trb.2017.02.004

Njus, E., 2016. How long can trains block railroad crossings? (Commuting Q&A) [WWW Document]. oregonlive. URL https://www.oregonlive.com/commuting/2016/11/how_long_can_trains_block_rail.html (accessed 8.1.22).

OenStreetMap, 2023. OpenStreetMap. Wikipedia.

OpenStreetMap [WWW Document], n.d. . OpenStreetMap. URL https://www.openstreetmap.org/ (accessed 5.24.23).

Park, P.Y., Jung, W.R., Yeboah, G., Rempel, G., Paulsen, D., Rumpel, D., 2016. First responders' response area and response time analysis with/without grade crossing monitoring system. Fire Safety Journal 79, 100–110. https://doi.org/10.1016/j.firesaf.2015.11.003

Patella, S.M., Grazieschi, G., Gatta, V., Marcucci, E., Carrese, S., 2021. The Adoption of Green Vehicles in Last Mile Logistics: A Systematic Review. Sustainability 13, 6. https://doi.org/10.3390/su13010006

Paul, T., Yamada, H., 2014. Operation and charging scheduling of electric buses in a city bus route network, in: 17th International IEEE Conference on Intelligent Transportation Systems (ITSC). Presented at the 17th International IEEE Conference on Intelligent Transportation Systems (ITSC), pp. 2780–2786. https://doi.org/10.1109/ITSC.2014.6958135

Phan, M.-H., Kim, K.H., 2015. Negotiating truck arrival times among trucking companies and a container terminal. Transportation Research Part E: Logistics and Transportation Review 75, 132–144. https://doi.org/10.1016/j.tre.2015.01.004

Poe, M.G. and M., 2018. Trains blocking roadway creates dangerous situations, first responders say [WWW Document]. KUTV. URL https://kutv.com/news/get-gephardt/trains (accessed 8.1.22).

Prodhon, C., Prins, C., 2014. A survey of recent research on location-routing problems. European Journal of Operational Research 238, 1–17. https://doi.org/10.1016/j.ejor.2014.01.005

Prohaska, R., Konan, A., Kelly, K., Lammert, M., 2016. Heavy-Duty Vehicle Port Drayage Drive Cycle Characterization and Development: Preprint (No. NREL/CP-5400-66649). National Renewable Energy Lab. (NREL), Golden, CO (United States). https://doi.org/10.4271/2016-01-8135

Salhi, S., Nagy, G., 1999. Consistency and Robustness in Location-Routing. Studies in Locational Analysis 3–19.

Salhi, S., Rand, G.K., 1989. The effect of ignoring routes when locating depots. European Journal of Operational Research 39, 150–156. https://doi.org/10.1016/0377-2217(89)90188-4

Sancho, N.G.F., 1994. Shortest Path Problems with Time Windows on Nodes and Arcs. Journal of Mathematical Analysis and Applications 186, 643–648. https://doi.org/10.1006/jmaa.1994.1324

Sandifur, M., 2021. Zero-emissions truck project launches at Port of Oakland [WWW Document]. Port of Oakland. URL https://www.portofoakland.com/press-releases/zero-emissions-truck-project-launches-at-port-of-oakland/ (accessed 10.9.23).

Saraiva, R.D., de Andrade, R.C., 2021. Constrained shortest path tour problem: models, valid inequalities, and Lagrangian heuristics. International Transactions in Operational Research 28, 222–261. https://doi.org/10.1111/itor.12782

Sassi, O., Cherif, W.R., Oulamara, A., 2014. Vehicle Routing Problem with Mixed fleet of conventional and heterogenous electric vehicles and time dependent charging costs.

Sassi, O., Cherif-Khettaf, W.R., Oulamara, A., 2015a. Iterated Tabu Search for the Mix Fleet Vehicle Routing Problem with Heterogenous Electric Vehicles, in: Le Thi, H.A., Pham Dinh, T., Nguyen, N.T. (Eds.), Modelling, Computation and Optimization in Information Systems and Management Sciences, Advances in Intelligent Systems and Computing. Springer International Publishing, Cham, pp. 57–68. https://doi.org/10.1007/978-3-319-18161-5_6

Sassi, O., Cherif-Khettaf, W.R., Oulamara, A., 2015b. Multi-start Iterated Local Search for the Mixed Fleet Vehicle Routing Problem with Heterogenous Electric Vehicles, in: Ochoa, G., Chicano, F. (Eds.), Evolutionary Computation in Combinatorial Optimization, Lecture Notes in Computer Science. Springer International Publishing, Cham, pp. 138–149. https://doi.org/10.1007/978-3-319-16468-7_12

Sassi, O., Oulamara, A., 2014. Joint Scheduling and Optimal Charging of Electric Vehicles Problem, in: Murgante, B., Misra, S., Rocha, A.M.A.C., Torre, C., Rocha, J.G., Falcão, M.I., Taniar, D., Apduhan, B.O., Gervasi, O. (Eds.), Computational Science and Its Applications – ICCSA 2014, Lecture Notes in Computer Science. Springer International Publishing, Cham, pp. 76–91. https://doi.org/10.1007/978-3-319-09129-7_6

SC Ports' volumes increase across business segments - SC Ports Authority [WWW Document], 2023. URL https://scspa.com/news/sc-ports-volumes-increase-across-business-segments/ (accessed 7.4.23).

Schambers, A., Eavis-O'Quinn, M., Roberge, V., Tarbouchi, M., 2018. Route planning for electric vehicle efficiency using the Bellman-Ford algorithm on an embedded GPU, in: 2018 4th International Conference on Optimization and Applications (ICOA). Presented at the 2018 4th International Conference on Optimization and Applications (ICOA), pp. 1–6. https://doi.org/10.1109/ICOA.2018.8370584

Schiffer, M., Walther, G., 2018. Strategic planning of electric logistics fleet networks: A robust location-routing approach. Omega 80, 31–42. https://doi.org/10.1016/j.omega.2017.09.003

Schneider, M., Stenger, A., Goeke, D., 2014a. The Electric Vehicle-Routing Problem with Time Windows and Recharging Stations. Transportation Science 48, 500–520. https://doi.org/10.1287/trsc.2013.0490

Schneider, M., Stenger, A., Goeke, D., 2014b. The Electric Vehicle-Routing Problem with Time Windows and Recharging Stations. Transportation Science 48, 500–520. https://doi.org/10.1287/trsc.2013.0490

Schrooten, L., De Vlieger, I., Panis, L.I., Chiffi, C., Pastori, E., 2009. Emissions of maritime transport: A European reference system. Science of The Total Environment 408, 318–323. https://doi.org/10.1016/j.scitotenv.2009.07.037

Sedeño-Noda, A., González-Martín, C., 2012. An efficient label setting/correcting shortest path algorithm. Comput Optim Appl 51, 437–455. https://doi.org/10.1007/s10589-010-9323-9

Sen, B., Ercan, T., Tatari, O., 2017. Does a battery-electric truck make a difference? – Life cycle emissions, costs, and externality analysis of alternative fuel-powered Class 8 heavy-duty trucks in the United States. Journal of Cleaner Production 141, 110–121. https://doi.org/10.1016/j.jclepro.2016.09.046

Shahram fard, S., Vahdani, B., 2019. Assignment and scheduling trucks in cross-docking system with energy consumption consideration and trucks queuing. Journal of Cleaner Production 213, 21–41. https://doi.org/10.1016/j.jclepro.2018.12.106

Soloveichik, G.L., 2011. Battery Technologies for Large-Scale Stationary Energy Storage. Annual Review of Chemical and Biomolecular Engineering 2, 503–527. https://doi.org/10.1146/annurev-chembioeng-061010-114116

Starcrest Consulting Group, L., 2022. 2021_Air_Emissions_Inventory.pdf.

Sun, X., 2020. Facilitating Cooperative Truck Platooning for Energy Savings: Path Planning, Platoon Formation and Benefit Redistribution (Thesis).

Tanvir, S., Un-Noor, F., Boriboonsomsin, K., Gao, Z., 2021. Feasibility of Operating a Heavy-Duty Battery Electric Truck Fleet for Drayage Applications. Transportation Research Record 2675, 258–268. https://doi.org/10.1177/0361198120957325

Teichert, O., Chang, F., Ongel, A., Lienkamp, M., 2019. Joint Optimization of Vehicle Battery Pack Capacity and Charging Infrastructure for Electrified Public Bus Systems. IEEE Transactions on Transportation Electrification 5, 672–682. https://doi.org/10.1109/TTE.2019.2932700

Teran, M.A., 2022. [Infographic] Series – Will heavy trucks go electric in North America? Part 1. The Big Challenge: Driving Rage. Mexicom Logistics. URL https://mexicomlogistics.com/electric-trucks-north-america-drigins-range/ (accessed 7.7.23).

Transportation (ICCT), I.C. on C., 2007. Air Pollution and Greenhouse Gas Emissions from Ocean-going Ships: Impacts, Mitigation Options and Opportunities for Managing Growth. Maritime Studies 2007, 3–10. https://doi.org/10.1080/07266472.2007.10878845

U.S. Bureau of Labor Statistics, J.C. and L., 2023. Charging into the future: the transition to electric vehicles : Beyond the Numbers: U.S. Bureau of Labor Statistics [WWW Document]. URL https://www.bls.gov/opub/btn/volume-12/charging-into-the-future-the-transition-to-electric-vehicles.htm#_edn2 (accessed 10.9.23).

U.S. Census Bureau, Department of Commerce, n.d. TIGER/Line Shapefile, 2019, nation, U.S., Rails National Shapefile.

US EPA, O., 2023a. Overview of Greenhouse Gases [WWW Document]. URL https://www.epa.gov/ghgemissions/overview-greenhouse-gases (accessed 10.9.23).

US EPA, O., 2023b. U.S. National Blueprint for Transportation Decarbonization [WWW Document]. URL https://www.epa.gov/greenvehicles/us-national-blueprint-transportation-decarbonization (accessed 7.4.23).

Wang, Y., Huang, Y., Xu, J., Barclay, N., 2017. Optimal recharging scheduling for urban electric buses: A case study in Davis. Transportation Research Part E: Logistics and Transportation Review 100, 115–132. https://doi.org/10.1016/j.tre.2017.01.001

Wen, M., Linde, E., Ropke, S., Mirchandani, P., Larsen, A., 2016. An adaptive large neighborhood search heuristic for the Electric Vehicle Scheduling Problem. Computers & Operations Research 76, 73–83. https://doi.org/10.1016/j.cor.2016.06.013

Whitehead, Jake, Whitehead, Jessica, Kane, M., Zheng, Z., 2022. Exploring public charging infrastructure requirements for short-haul electric trucks. International Journal of Sustainable Transportation 16, 775–791. https://doi.org/10.1080/15568318.2021.1921888

Wu, X., Zhang, Y., Chen, Y., 2023. A Dynamic Programming Model for Joint Optimization of Electric Drayage Truck Operations and Charging Stations Planning at Ports. IEEE Transactions on Intelligent Transportation Systems 1–10. https://doi.org/10.1109/TITS.2023.3285668

Yang, J., Sun, H., 2015. Battery swap station location-routing problem with capacitated electric vehicles. Computers & Operations Research 55, 217–232. https://doi.org/10.1016/j.cor.2014.07.003

Yeun, L.C., Ismail, W.R., Omar, K., Zirour, M., 2008. VEHICLE ROUTING PROBLEM: MODELS AND SOLUTIONS. Journal of Quality Measurement and Analysis JQMA 4, 205–218.

You, S.I., Ritchie, S.G., 2018. A GPS Data Processing Framework for Analysis of Drayage Truck Tours. KSCE J Civ Eng 22, 1454–1465. https://doi.org/10.1007/s12205-017-0160-6

Young, K., Wang, C., Wang, L.Y., Strunz, K., 2013. Electric Vehicle Battery Technologies, in: Garcia-Valle, R., Peças Lopes, J.A. (Eds.), Electric Vehicle Integration into Modern Power Networks, Power Electronics and Power Systems. Springer, New York, NY, pp. 15–56. https://doi.org/10.1007/978-1-4614-0134-6_2

Yu, G., Yang, J., 1998. On the Robust Shortest Path Problem. Computers & Operations Research 25, 457–468. https://doi.org/10.1016/S0305-0548(97)00085-3

Zhang, D., Zhan, Q., Chen, Y., Li, S., 2018. Joint optimization of logistics infrastructure investments and subsidies in a regional logistics network with CO2 emission reduction targets. Transportation Research Part D: Transport and Environment, Special Issue on Traffic Modeling for Low-Emission Transport 60, 174–190. https://doi.org/10.1016/j.trd.2016.02.019

Zhang, Z., Liu, X., Holt, K., 2020. Prevention of End-of-Track Collisions in Passenger Terminals via Positive Train Control: Benefit-Cost Analysis and Operational Impact Assessment. Transportation Research Record 2674, 16–28. https://doi.org/10.1177/0361198120920628

Zhao, L., Zhao, J., 2017. Comparison Study of Three Shortest Path Algorithm, in: 2017 International Conference on Computer Technology, Electronics and Communication (ICCTEC). Presented at the 2017 International Conference on Computer Technology, Electronics and Communication (ICCTEC), pp. 748–751. https://doi.org/10.1109/ICCTEC.2017.00165

Zhen, L., Ma, C., Wang, K., Xiao, L., Zhang, W., 2020. Multi-depot multi-trip vehicle routing problem with time windows and release dates. Transportation Research Part E: Logistics and Transportation Review 135, 101866. https://doi.org/10.1016/j.tre.2020.101866

Zuo, X., Xiao, Y., You, M., Kaku, I., Xu, Y., 2019. A new formulation of the electric vehicle routing problem with time windows considering concave nonlinear charging function. Journal of Cleaner Production 236, 117687. https://doi.org/10.1016/j.jclepro.2019.117687

APPENDIX A

SUPPLEMENTARY TABLES

Table A.1 Distance matrix for the highway system in the southeastern United States. (Unit: km)

	6	43	94	103	187	191	205	243	245	320	337	338	…	543
6	-			134				173	213					
43		-				98								
94			-											
103	134			-				39			238			
187					-	34				96				
191		98			34	-								
205							-					112		
243	173			39				-	40					
245	213							40	-					
320					96					-				
337				238							-			
338							112					-		
⋮													⋱	⋮
543													...	-

Table A.2 Travel time matrix for the highway system in the southeastern United States. (Unit: hour)

	6	43	94	103	187	191	205	243	245	320	337	338	…	543
6	-			2.2				2.8	3.4					
43		-				1.6								
94			-											
103	2.2			-				0.6			3.5			
187					-	0.6				1.5				
191		1.6			0.6	-								
205							-					1.8		
243	2.8			0.6				-	0.6					
245	3.4							0.6	-			2.45		
320					1.5					-				
337				3.5							-			
338							1.8		2.45			-		
⋮													⋱	⋮
543													...	-

Table A.3 Coordinates for nodes in the road network of the City of Columbia.

Index	ID	Longitude	Latitude
1	1022590762	-81.07765418	33.97007430
2	1022590774	-81.07813520	33.97026917
3	113357821	-80.78291696	34.11869371
4	113386469	-81.12501302	33.99286802
5	113386513	-81.12388799	33.99313900
6	113386522	-81.11067599	33.96374803
7	113386548	-81.10896503	33.96399902
8	113386568	-81.08788998	33.98728107
9	113386571	-81.08894600	33.98889299
10	113386577	-81.08662103	33.98532901
11	113386579	-81.08748400	33.98667601
12	113386804	-81.05122796	33.98468396
13	113386807	-81.05180233	33.98453130
14	113386844	-81.07122404	33.94268700
15	113386848	-81.07124601	33.94192001
16	113388444	-81.13605002	33.99326604
17	113388446	-81.13608095	33.99297406
18	113388461	-81.13665994	33.99089501
19	113388463	-81.13748901	33.99036305
20	113388656	-81.14604648	34.07074536
21	113389145	-81.05781678	33.92983914
22	113389191	-81.06819453	33.92998301
23	113390024	-81.11442103	34.04065805
24	113390376	-81.15044274	34.01287667
25	113390460	-81.15356302	34.00943707
26	113390527	-81.14603904	33.99521900
27	113390530	-81.14626296	33.99654208
28	113390605	-81.14681204	33.99634300
29	113391064	-81.05946501	33.91996405
30	113391067	-81.06049899	33.92081008
31	113391071	-81.06001404	33.92149603
32	113391073	-81.05951099	33.92120803
33	113391089	-81.05965594	33.91931703
34	113391137	-81.05556897	33.99524902
…	…	…	…
1128685	cluster_931214226_931214408	-80.96467576	33.9936477

Table A.4 Edges in the road network of the City of Columbia.

ID	From	To	Priority	Length(m)	Speed(m/s)
-107459657#0	114000062	2533686122	3	376.29	13.89
-107459657#1	114000076	114000062	3	280.15	13.89
-107459657#2	114000089	114000076	3	658.30	13.89
-107459657#3	114000096	114000089	3	168.43	13.89
-107459657#4	113998916	114000096	3	124.75	13.89
-107459657#5	113996701	113998916	3	156.02	13.89
-107459868#1	114043490	114043473	3	341.51	13.89
-107459868#3	114000076	114043490	3	185.62	13.89
-107738516#0	1237711187	4728280298	3	26.72	13.89
-107738516#1	3528575322	1237711187	3	33.35	13.89
-107738516#2	1237711140	3528575322	3	17.18	13.89
-108135223	114004674	113492041	3	61.21	13.89
-108349185#0	114033727	114000089	3	243.63	13.89
-108349185#1	114053124	114033727	3	141.98	13.89
-108349185#4	113963770	114053124	3	152.12	13.89
-109771861	114028697	114084745	10	157.33	22.22
-110337070#0	3574885198	1260283322	3	276.84	13.89
-110337070#1	5265161977	3574885198	3	56.29	13.89
-110450199#1	113955985	114071153	12	46.34	27.78
-113712180#0	1289125043	1289125020	3	38.50	13.89
-113712180#1	5321003354	1289125043	3	127.30	13.89
-113712182	1289125018	1289125070	3	22.28	13.89
-113712183	1289125051	6427139458	3	177.18	13.89
-113712184#0	1289125075	1289125022	3	22.53	13.89
-113712184#1	1289125185	1289125075	3	34.03	13.89
-113712186#0	1289125043	1289125108	3	206.53	13.89
-113712186#1	1289125071	1289125043	3	217.29	13.89
-116159470#1	114019134	114019132	3	141.48	13.89
-116159470#2	113992903	114019134	3	143.47	13.89
-116159475#1	113992907	113992903	3	140.71	13.89
-116159475#2	113992910	113992907	3	165.42	13.89
-117699767	1325484065	114019248	3	190.17	13.89
-119994706#0	6568565430	1346548758	12	36.65	27.78
-119994706#1	114101158	6568565430	12	128.77	27.78
-119994707#4	2534251735	114101158	12	232.09	27.78
⋮	⋮	⋮	⋮	⋮	⋮
87968497	1022590774	1022590762	7	44.69	22.22

Table A.5 Coordinates for grade crossings in the City of Columbia.

ID	Longitude	Latitude	Affected road node ID
1303	-81.0215	33.99423	113982748
1331	-81.0254	33.97797	113983454
1332	-81.0247	33.97938	113983456
1414	-81.0055	34.05195	113985704
1415	-81.0075	34.05275	113985706
1716	-81.0199	34.04631	113994000
1728	-81.0189	33.99831	113994312
1730	-81.0225	34.00926	113994337
1734	-81.0338	33.98729	113994464
1998	-80.9735	34.08684	114000244
2146	-81.0548	34.00764	114003667
2944	-81.0349	34.03784	114025744
3234	-80.9992	34.05789	114033363
3242	-80.9825	34.0671	114033393
3650	-81.0297	33.98822	114046104
3716	-81.0259	33.98557	114047897
3887	-81.0279	34.04178	114051648
3995	-81.0226	33.99316	114056054
4066	-81.019	33.97947	114058778
5353	-81.0745	34.01064	1836079196
5355	-81.0304	33.98996	1836818367
5439	-80.9556	33.96827	2428685874
6348	-81.0186	33.99967	3139383921
6523	-81.0231	34.01055	3639960420
7005	-81.0225	33.98127	5884204355
7062	-81.0261	33.98849	6236360687

Table A.6 Distance matrix for the road network in the City of Columbia. (Unit: meter)

	0	1	2	3	4	5	6	7	8	9	10	11	…	7667
0	-	45												
1	45	-												
2			-	169										
3			169	-										
4					-	56								
5					56	-								
6							-	88						
7							88	-						
8									-	85				
9									85	-				
10											-	74		
11											74	-		
⋮													⋱	⋮
7667													...	-

Table A.7 Distance matrix for the railroad network in the City of Columbia. (Unit: meter)

	0	1	2	3	4	5	6	7	8	9	10	11	…	64
0	-	100												
1	100	-	560											
2		560	-	160										
3			160	-	320									
4				320	-	180								
5					180	-	680							
6						680	-	160						
7							160	-	740					
8								740	-	200				
9									200	-	560			
10										560	-	160		
11											160	-		
⋮													⋱	⋮
64													...	-

APPENDIX B

COPYRIGHT PERMISSION

The paper entitled “A Dynamic Programming Model for Joint Optimization of Electric Drayage Truck Operations and Charging Stations Planning at Ports”:

Please note that, as the author of this IEEE article, you retain the right to include it in a thesis or dissertation, provided it is not published commercially. Permission is not required, but please ensure that you reference the journal as the original source.